

Public Final Report



ESPRIT – Project №: 33915

Long Term Research

MINIMAN

Miniaturised Robot for Micro Manipulation

Report №: 3

Contract start date: 01-Nov-1998

Contract termination date: 31-Jan-2002

Editor, Co-ordinator

University of Karlsruhe, Institute for Process Control and Robotics, Karlsruhe,
Germany

IPR

Authors - Academic Partners

Fraunhofer Gesellschaft, Fraunhofer Institute for Biomedical Engineering,
St. Ingbert, Germany

IBMT

Scuola Superiore Sant'Anna, MiTech Lab, Pisa, Italy

SSSA

University of Barcelona, Instrumentation and Communication Systems
Laboratory, Barcelona, Spain

SIC

Sheffield Hallam University, School of Engineering, Sheffield, Great Britain

SHU

Uppsala University, Department of Materials Science, Uppsala, Sweden

DMS

Authors - Industrial Partners

Philips Electronics Nederland bv., Philips Research Laboratories, Eindhoven,
The Netherlands

PRLE

Kammrath & Weiss GmbH, Dortmund, Germany

K&W

Report Preparation Date: 22-March-2002

Classification: Public

Contents

1. PROJECT OVERVIEW	3
1.1 Summary	3
1.2 The Miniman Consortium	3
1.3 Main Achievements	4
2. PROJECT OBJECTIVES	4
3. METHODOLOGIES	5
3.1 Workpackage 1: Microrobots	5
3.1.1 Miniman III/IV System (D101 and D103)	5
3.1.2 Miniman V System (D102)	7
3.2 Workpackage 2: Grippers and Tools	9
3.2.1 Cell Handling	9
3.2.2 Handling of Mechanical Parts	11
3.2.3 Handling Techniques inside the SEM	14
3.3 Workpackage 3: Sensors	15
3.3.1 Task 3.1: Force Sensors	15
3.3.2 Task 3.2: Tactile Sensors	18
3.3.3 Task 3.3: Vision Sensors (Position Detection)	21
3.3.4 Summary	28
3.4 Workpackage 4: Control System	28
3.4.1 Task 4.1: Computer System	28
3.4.2 Task 4.2: Power Electronic Circuits (Deliverable D405)	29
3.4.3 Task 4.3: Interface for Telemanipulation	30
3.4.4 Task 4.4: Control Algorithms	31
3.4.5 Task 4.5: Environment for Semi-Automated Manipulation	32
3.5 Workpackage 5: System Integration and Demonstrations	32
3.5.1 Task 5.1: Hardware Integration	33
3.5.2 Task 5.2: Software Integration – Miniman III/IV System	35
3.5.3 Demonstration Tasks 5.3, 5.4 and 5.5	36
4. PROJECT ACHIEVEMENTS – EVALUATION OF MINIMAN	36
4.1 Miniaturised prototype Miniman V	36
4.2 DEM1: Assembly of a Micro Lens System	38
4.2.1 The Gel-Pak	39
4.2.2 Transferring the subassembly to the LAU	40
4.2.3 Mounting the main lens	40
4.2.4 Alignment of the lens system	41
4.2.5 Results	41
4.3 DEM2: Handling Tasks inside the SEM	42
4.4 DEM3: Cell Handling	43
4.4.1 Hardware used for cell handling	44
4.4.2 Demonstration procedure	44
4.4.3 Results	45
4.5 Additional Subsystems	46
4.5.1 Force Feedback	46
4.5.2 Tactile Microsensor	46
4.6 Benefits to Society	47
4.7 Conclusion	48
5. EXPLOITATION: EVENTUAL COMMERCIALISATION OF MINIMAN	49
5.1 Definition of the “Product”	49
5.2 Biological applications	49
5.3 Mechanical applications under the light microscope	50
5.4 SEM applications	50
6. DELIVERABLES	51
7. REFERENCES	52
8. OUTLOOK	54

1. Project Overview

1.1 Summary

The field of micromanipulation and microrobotics is still in its initialisation stage and industrial activities today focus on the creation of manipulation and assembly facilities which are tailored to a specific task. The major motivation for carrying out this project was the lack of adequate micromanipulation systems for a wide variety of applications – ranging from a high-precision assembly of mechanical microcomponents in industry to the handling of cells in medical or biological applications.

The main idea of the Miniman project is the development of a smart microrobot with 5 degrees of freedom and a size of a few cm³, capable of moving and manipulating by the use of tube-shaped and multilayered piezo-actuators. Controlled by visual and force/tactile sensor information, the microrobot is able to perform manipulations with a motion resolution down to 10 nm in a telemanipulated or semi-automated mode, and so it will free humans from the tedious task of having to handle minuscule objects directly. Equipped with micromachined grippers, the robot can take over high-precise grasping, transport, manipulation and positioning of mechanical or biological micro-objects, under a light microscope or within the vacuum chamber of a scanning electron microscope. A powerful computer system using inexpensive PC-compatible hardware components ensures the robot operation in real-time.

The flexibility of the Miniman concept due to the integration of positioning and manipulating units into a microrobot will be of great interest for different industrial users. However, there is a gap between the needs of the industry attempting to take-up the achievements of microsystem technology and to take a lot of different miniaturised products to the market and the performance of the existing approaches for micromanipulation. To come up to the high expectations for advanced micromanipulation systems, a longer term industrial vision is necessary. The Miniman collaboration, including well established European research institutes and companies, contributes to solve this problem. The academic partners are among the leading European institutes in the field of microsystem technology and advanced robot systems. The industrial partners have been active in the field of micromanipulation and microassembly.

The performance of the Miniman microrobot is demonstrated by means of the following demonstrations which have been specified in the project programme:

- 1) handling and assembly of micromechanical parts under a light microscope,
- 2) handling of micromechanical parts in the vacuum chamber of a scanning electron microscope (SEM)
- 3) grasping, moving and sorting of biological cells under an optical microscope.

All three application fields are very different in terms of dimension or nature of the objects to be handled and in terms of operating environment, hence they demonstrate the flexibility of the Miniman system.

To summarise, the Miniman approach does not have immediate short-term market expediency but is expected to lead to an innovative micromanipulation technology with a clearly identifiable route for its take-up by industry. Moreover, the development of the individual microrobot components is additionally delivering a lot of new information and understanding for further promising technologies and neighbouring application fields.

This report describes the results of the work carried out by the whole Consortium in the three years of the project's duration. It will give an outlook on the possible take-up and dissemination of the results and conceivable research topics rooting in the promising results of the Miniman project.

1.2 The Miniman Consortium

The Miniman Consortium consists of six academic and two industrial partners. The project co-ordinator is the Institute for Process Control and Robotics of the University of Karlsruhe in Germany (*IPR*). IPR is one of the leading institutes for robot control and process automation in Germany. In the Miniman project, IPR has developed the control system – both hard- and software – for the micro-robots driven by tube-shaped piezos. Beside the co-ordination work, also a large amount of the integration work has been performed in Karlsruhe, since the demonstration systems have been set up there.

The Departament d'Electrònica of the University of Barcelona in Spain (*SIC*, which were abbreviated *EME* in the project programme) made the very high integration of control and high voltage electronic circuitry possible and was responsible for the development of the Miniman V robot together with the Swedish partner DMS.

The Department of Materials Science of Uppsala University in Sweden (*DMS*) has developed low-voltage multi-layered piezo elements which are employed in the Miniman IV and V robots. The low-voltage drive and compact actuator design have made further miniaturisation and integration possible.

The Institute for Biomedical Engineering of the Fraunhofer Gesellschaft in St. Ingbert, Germany (*IBMT*) acted both as a user and as a supplier in the Miniman project. IBMT has developed a tactile sensor array which can be integrated into endeffectors of micro-robots to get information on gripping and contact states between the gripper and the object to be gripped. At the same time, the IBMT acted as a user by specifying the cell manipulation demonstrator.

The School of Engineering of the Sheffield Hallam University in Great Britain (*SHU*) has developed computer vision systems for micro-manipulation tasks. These vision systems can recognise micro-objects such as biological cells, robot endeffectors or micromechanical parts. This data is used for the closed-loop control of the micro-robots in semi-automated mode.

The MiTech Lab of the Scuola Superiore Sant' Anna in Pisa, Italy (*SSSA*) focused on the development of robot end-effectors with integrated force sensors, force feedback telemanipulation user interfaces and techniques for handling micromechanical parts.

The role of Philips Research Laboratories of the Nederlandse Philips Bedrijven B.V. in Eindhoven, The Netherlands (*PRLE*) has been the one of a user. They have specified the micromechanical demonstration and provided valuable advice for the project from an industrial point of view.

The Kamrath & Weiss GmbH in Dortmund, Germany (*K&W*) are a supplier of high precision equipment for scanning electron microscopy (SEM) and supplied components for the robot system as well as the specifications for the SEM demonstration.

1.3 Main Achievements

The project's main achievements can be summarised as follows:

- the development of a cm³-sized micro robot with integrated control circuits
- the development of low-voltage multilayered piezo actuators which can be applied in various micromechanical systems demanding for low-voltage drives with the advantages of piezo elements
- development of hybrid circuitry for piezo elements which needs only a minimal set of wires and can generate driving voltages for piezo elements onboard a micro system
- a variety of components which enhance the feasibility of micro manipulation – ranging from endeffectors, force and tactile sensors to gripper systems for both micromechanical and biological specimens – and
- their integration in a flexible microrobot system resulting in a essential tool for very different micro manipulation tasks
- a profound understanding of micro processes in various orders of magnitude, including computer vision and control issues.

2. Project Objectives

As stated in the project programme, the project's success can be measured against the following list of objectives:

- Development and specification of the handling techniques required
- Development of microrobots driven by tube-shaped and/or multilayered piezoactuators, consisting of a micropositioning unit and a micromanipulating unit
- Development of piezo-driven grippers and suction tools for operating with micromechanical parts and with biological objects, especially biological cells
- Development and fabrication of a force microsensor and a tactile microsensor, which can be integrated into the developed grippers and used in the applications defined in the project
- Development of a computer vision system to locate and control the microrobots
- Development of an interface for telemanipulated control of a microrobot system to transform the operator's hand motion into the 3D motion of the microrobots by means of a joystick or mouse

- Development of an easily understandable graphical user interface providing the operator with the information needed for a telemanipulated or semi-automated control of a microrobot system
- Development of closed-loop control algorithms for the position/force control of a microrobot, based on the information delivered by the sensors of the microrobot system
- Development of a powerful computer system employing standard PC-compatible hardware components, in order to ensure the microrobots' operation in real-time
- Development of high voltage electronic control circuits to drive the piezoactuators of a microrobot, optimising size, weight and cost of the microrobot system
- Development and preparation of demonstrations to evaluate the abilities of the microrobots by the (partial) assembly of several highly miniaturised test products provided by Philips
- Development and preparation of a demonstration to evaluate the abilities of the microrobots by sorting biological cells within microcuvettes
- Analysis of the resulting micromanipulation processes in all the prepared demonstrations. The performance of the microrobots will be evaluated and a specification of measures needed for further system adaptation and optimisation will be done.

3. Methodologies

This chapter provides a description of the work carried out within each of the five project's workpackages. It also includes design alternatives considered by the Consortium.

3.1 Workpackage 1: Microrobots

The goal of Workpackage 1 was the development of the hardware of the flexible mobile microrobots the Miniman project bases on. All Miniman robot prototypes consist of a mobile positioning unit with two translatory and one rotational degree of freedom (DOF), which carries a manipulation unit with a micro tool. Two types of microrobot drives have been developed. While the relatively large decimetre-sized prototypes Miniman III and IV are driven by tube-shaped piezo elements, the Miniman V robot bases on multilayered piezo actuators. The requirements on all Miniman robots are high operation speeds of 30 mm/s and 45°/s on the one hand and a high motion resolution of 10 nm on the other.

Miniman III and IV are employed in the three Miniman demonstrators under the light microscope and inside the vacuum chamber of the scanning electron microscope. All tools and sensors required for the realisation of these demonstrators are integrated in robots of this type.

Miniman V is the final, fully miniaturised Miniman robot. Being only a few cm³ small it has its electronic circuits on-board and represents the future potential of the Miniman system.

Additionally, the platform of Miniman IV was used to demonstrate the combination of both driving principles in one robot.

Workpackage 1 was divided into two tasks:

Task 1.1: Development of Micropositioning Units

Task 1.2: Development of Micromanipulating Units

In the following paragraphs, which are divided by robot types, these two tasks will be treated together, because for each robot type the positioning and the manipulating units base on the same driving principles.

3.1.1 Miniman III/IV System (D101 and D103)

The positioning units of the prototypes Miniman III and IV are driven by three tube-shaped piezo-legs using a slip-stick principle as explained in [Breguet 96]. It combines high resolution with high performance, small size and high flexibility. Therefore it is an established driving principle in microrobotics and also employed in other important microrobot projects as *e.g.* the "Nanowalker" (MIT, [Martel 01]). The outer electrode of these piezoelements is divided into four parts. By applying voltages (± 150 V) between one or more of the outer electrodes and the inner one, the legs can be bent in all directions causing the robot to move within an area of ca. $4 \times 4 \mu\text{m}^2$. The achievable resolution of this "scan" or "sneak" mode is ca. 10 nm. In order to let the robot "walk" over larger distances, a series of microsteps is performed. First, the robot is displaced in the desired direction by bending the piezolegs. When the voltage is abruptly changed afterwards, the piezolegs are bent in the opposite

direction very quickly and the robot's feet (small ruby spheres) slip over the surface of the working base because of the robot's inertia. The step is completed after relaxing the piezolegs to the upright position and the next one can follow. By applying the corresponding saw tooth voltage with high frequencies, speeds of up to 30 mm/s were reached. This meets the requirements defined in the project programme. However, the maximum speed of the robots is usually lower, because it is strongly dependent on various parameters such as the quality of the surface and the weight of the robot. In the Miniman demonstrations it is only relevant to the global positioning of the robot, *i.e.* when the robot is not moving within the field of view of the microscope. As this global motion is limited by the global sensor system anyway, no more efforts were taken for guaranteeing this maximum speed.

The manipulation unit of Miniman III consists of a polished steel or aluminium sphere with a diameter of 30 mm. The robot's endeffector, *e.g.* a microgripper, is attached to this sphere. The sphere lies on three piezolegs that are fixed to the positioning unit. When these piezolegs "walk" across the sphere's surface, their bending and stepping cause the sphere to turn. Accordingly, the endeffector can be positioned with three DOF. Together with the three DOF of the positioning unit, Miniman III has five DOF, since one axis – the yaw axis – is redundant.

According to the special tasks of Miniman III different tools as micro-grippers or micro-pipettes (see Chapter 3.2, page 9) are integrated in such a sphere, which can be manually exchanged very easily. Being not required for the Miniman Demonstrators the implementation of an *automatic* tool exchange had to be renounced in favour of more important tasks.

The Miniman III and IV prototypes are equipped with infrared LEDs that enable the global positioning system (see Chapter 3.3.3.1, page 21) to detect the coarse position of the robots.

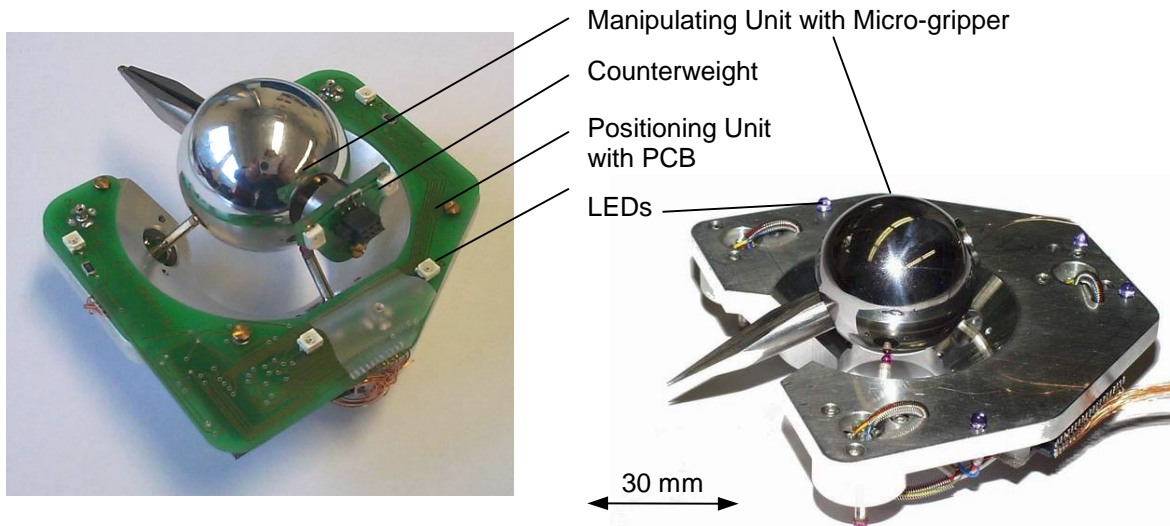


Figure 1: The Miniman III prototypes: Miniman III-2 (left) and the older Miniman III-1 (right) with SEM gripper

Figure 1 shows the Miniman III prototypes. After the realisation of the first one – Miniman III-1, **Deliverable D101** – the design was slightly changed when two more robots of the so called Miniman III-2 type were manufactured. A crucial problem of Miniman III-1 is the connection of the robot to the control system. Since the robots do not carry any electronics themselves, they need up to 50 electrical connections (see lower right of Figure 1).

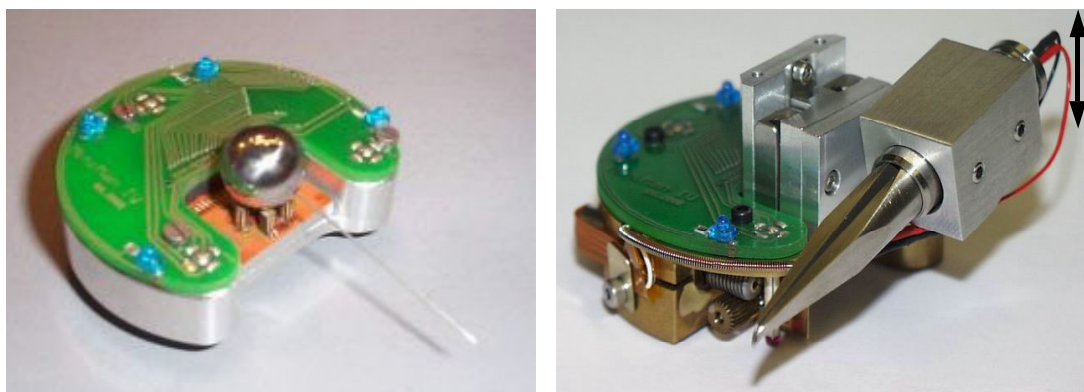


Figure 2: Miniman IV

As a consequence, long flexible printed circuit “boards” were developed replacing bundles of single thin wires. This technology was also used for the Miniman IV prototypes. For Miniman III-2 and Miniman IV printed circuit boards were developed for the connection of the piezo actuators and the LEDs. The principle of the manipulating unit of Miniman III-2 is similar to that of Miniman III-1. Figure 2 shows different versions of the Miniman IV prototypes. The left image shows the combination of the driving principles based on tube-shaped and multilayered piezo actuators in one robot (**Deliverable D103**). In this case the manipulating unit is similar to that of Miniman V (see below). It is connected to the main printed circuit board of Miniman IV. In the SEM demonstration, Miniman IV acts as a second robot being a helping hand when manipulating smallest particles. For this purpose, a conventional linear z-drive were developed as alternative manipulator for Miniman IV. Its miniature motor is integrated in the robot’s body and connected via the same printed circuit board (Figure 2, right).

3.1.2 Miniman V System (D102)

3.1.2.1 Design and fabrication strategy

Contemporary microrobots are either based on silicon MEMS technology or more conventional fabrication techniques. The present work is based on a new fabrication technique for piezoceramic actuators that gives a better freedom in design. The more advanced MEMS robots are mobile and can carry load, but do not have the ability to high precision motion. The presented solutions of the more conventional approaches do not provide enough flexibility, miniaturisation potential or motion precision. Common for all is that the selection of actuator material and motion mechanism is crucial. The actuator has to give enough mobility, precision, force (torque), speed and reliability. At the same time the actuator should be cheap to fabricate and looking into the future the technique has to allow for further miniaturisation. Piezoceramic materials are well suited for microactuator applications and the most promising miniaturised robots are based on piezoceramics. The material is able to generate very precise small motions and due to an inherent high stiffness, high forces can be transferred. The material can also be operated at high frequencies, making it possible to get a high working speed. Tube actuators, bimorphs and other kind of arrangements significantly improve the small intrinsic movements of the material, and to produce a motion with a theoretically unlimited working range, different step repetition mechanisms can be used, e.g. stick-slip, inch-worm and resonant techniques. The stators presented in this paper have been designed for a quasi-static walking mechanism mimicking the motion of a six-legged insect, but also other motion mechanisms can be used which makes it possible to make comparisons between different mechanisms. To get a static stability of a robot platform, only three legs are necessary. Using such a platform, motion mechanisms utilizing the inertia or resonance of moving parts have to be used. Most common are platforms with three piezoceramic actuators, which use an inertial driving mechanism, e.g. stick-slip. Similar systems using such platforms are the Nano-Walker developed by the MIT and microrobots developed by EPFL in Lausanne. Miniman III is another example. Locomotion is achieved in an easy way without special requirements on the design or fabrication technique. Miniaturisation will of course result in reduced mass of the moving parts, which eventually will cause problems when surface related effects, e.g. adhesive forces, become more important. Using a quasistatic walking mechanism for the miniature robots several envisioned problems should be possible to reduce. The six-legged stator allows for such a motion mechanism, but the complexity in the design, fabrication and locomotion is increased. The position control should be better when using the quasi-static mechanism than using an inertial mechanism, but this has to be further evaluated.

Piezoceramic actuators require high electric fields to attain a useful strain. High voltage, in the kV range, is needed for components with mm-spacing between electrodes while we had to use multilayer structures to reduce the drive voltage to levels common for integrated circuits. Multilayer actuators are usually fabricated by lamination of single tape cast ceramic layers with screen-printed electrodes. Single components are most often diced out in the green ceramic state. Thus, the geometrical freedom in the design is strictly limited. A new shaping process for multilayer piezoceramic components has been developed to overcome the geometrical limitations. The piezoceramic structures in Miniman V are fabricated with a wet building process, known from manufacturing of multilayer ceramic capacitors, where thin layers of ceramic slurry and screen-printed electrodes are cast sequentially. Thereafter a high precision CNC micro milling machine is used to shape the components.

3.1.2.2 Microrobot design

The microrobot consists of two monolithic piezoceramic stator units, put together back to back, Figure 3. The lower one, the positioning unit, can move in two orthogonal directions on a flat surface and rotate around the surface normal direction. The upper one, the manipulating unit, can rotate a ball around three orthogonal directions. A tool, which may be designed for a specific application, is attached to the ball.

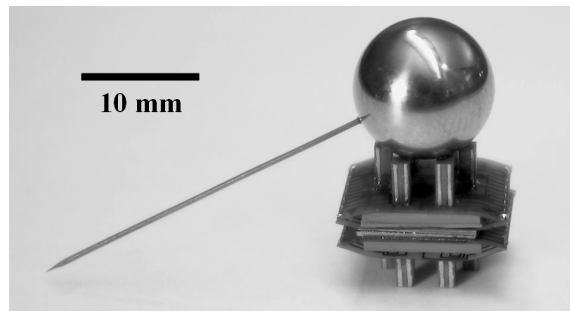


Figure 3: First demonstrator of a miniaturised robot for micromanipulation. Two piezoceramic stator units are put together back to back. One stator is intended for lateral movements on a flat surface and the other for rotating a ball arbitrarily.

Each stator unit has six legs, which each move in three orthogonal directions. The six legs are integrated on the base and their centres are placed with the same distance from the centre of the stator. The only difference between the positioning unit and the manipulating unit is the shape of the top surface of the legs. Initially legs with planar top surfaces, equal in size with the legs, were evaluated but due to various edge effects another design was chosen. The positioning unit got a robust pyramidal design, whereas the leg tips of the manipulating unit have sharp rounded tips to improve the contact with the ball.

The legs act as bimorphs, but they are different from piezoceramic bimorphs used in earlier presented piezoelectric motors. The electrode pattern of each leg in this design is divided into four electrically separated quadrants, Figure 4. There is a spacing of $200\ \mu\text{m}$ between the electrodes to avoid short circuits between phases. Every other electrode layer is a common ground layer. The internal electrodes are connected to external electrodes on the sidewall of the multilayer component. To minimise risks for short circuits a further spacing of $200\ \mu\text{m}$ between the internal electrodes and the external electrode to which they are not connected was chosen in the design.

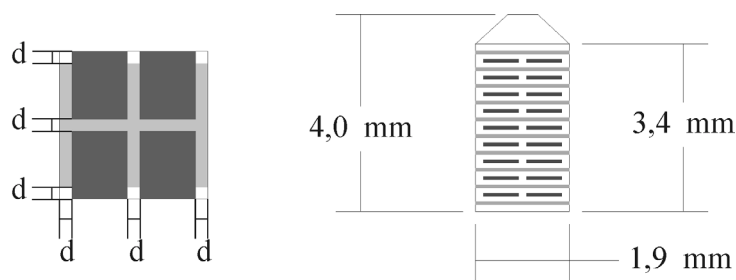


Figure 4: (left) The electrode pattern seen from above, the four phases are dark grey and the earth layers are light grey. Spacing between electrodes, $d=0.2\ \text{mm}$. (right) Cross section of a leg showing the alternating phase and earth electrode layers.

The legs can be bent in any direction depending on the amplitude of the applied voltage in the quadrants, making a 3-axial movement possible. The tip movement is confined to a rhombic area. Within this area, the tip can move along essentially any desired trajectory with properly chosen waveforms and phases of the drive voltages supplied to the bimorph.

Dividing the six legs into two independent sets, a walking mechanism can be obtained. The waveforms of the drive voltage for the two sets are phase shifted by 180° . During a walking step, three elements are in friction contact with the counter-surface and movements can be made arbitrarily short and slow, if the resolution in the drive signal is unlimited. Using 3-axial actuators in this six-leg configuration, and having two stator units make it possible to get a 5-axial movement of the tool. Driving the two sets in phase makes different inertial mechanisms, like stick-slip, possible.

The driving voltage should preferably be low and $50\ \text{V}$ is a feasible level for integrated circuits. To achieve a reasonable piezoelectric strain, the layer thickness should be in the order of $100\ \mu\text{m}$ or less. A reduction in the layer thickness reduces the yield as well, and a reasonable compromise is to choose $40\ \mu\text{m}$ as target value. An application specific integrated circuit (ASIC) has been designed to control four of the 24 phases in a stator unit. This integrated circuit contains 4 voltage power drivers and a digital control system with a fast serial interface protocol. A first assembling of 6 of these ASIC's has been carried out on a $21 \times 21\ \text{mm}^2$ printed circuit board (PCB) board in order to validate the system. In the first prototype a compact assembly process is shown, Figure 3, where the ASICs are intended to be mounted with flip chip bonding onto the same flexible printed circuit

(FPC) that connects to the legs of both stator units. There are only six wires to the robot, three for control information and three for power supply.

3.1.2.3 Fabrication of piezoceramic stator units

The multilayer structures have been fabricated by a wet building process. Ceramic slurry, which is a suspension of piezoceramic powder in a solution of polymer binder, dispersant and a solvent, is cast in a thin layer onto a glass plate with a doctor blade. After drying an electrode layer is deposited with screen-printing on top of the ceramic layer. A second ceramic layer can be deposited as soon as the electrode layer has dried. In such a way ceramic layers and electrode layers are alternately deposited until the full component height is reached. The green multilayer structure is machined to single components using a high precision CNC micro-milling machine, the polymer binder is burned out and the material is sintered at high temperatures. External electrodes, connecting the internal electrodes, are deposited on the sidewalls of the legs. Finally, the tips of the legs are polished to obtain a good fitting to the counter surface.

To prepare the ceramic slurry, a ceramic powder with a grain size of 1.5 μm in solution with dispersant and toluene is ball milled for 16 hours. After addition of polymer binder and another hour ball milling, the ceramic slurry is passed through a fabric with a mesh opening of 50 μm . Ceramic layers are cast without internal electrodes to a height of 1.85 mm. Thereafter, patterned Pt-electrodes are screen printed on top of every ceramic layer to a total height of 6.00 mm. Screen printing is performed using a woven polyester screen, which is aligned to the green body with guide pins. Pt-paste is applied manually with a squeegee. Finally, ceramic layers are cast without internal electrodes to the full height, 7.00 mm. The individual layer thickness is 50 μm throughout the whole green body. A high precision CNC micro milling machine equipped with a double-edged end mill ($\text{\O} 1.5 \text{ mm}$) is used to cut out components from the green body.

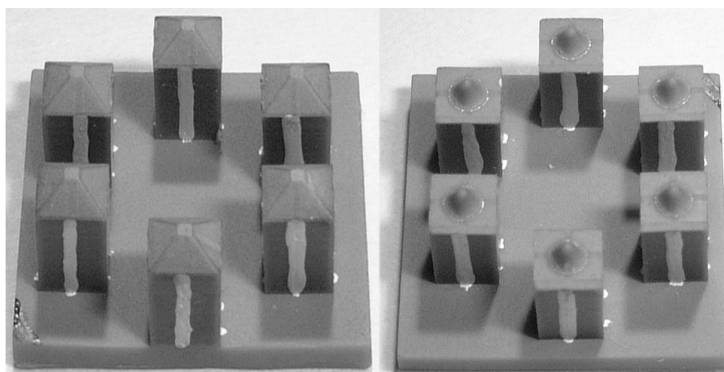


Figure 5: Six-legged monolithic piezoceramic positioning and manipulating units.

3.2 Workpackage 2: Grippers and Tools

Workpackage 2 is divided in two tasks: Task 2.1, Handling Techniques and Task 2.2, Application Specific Design. Since handling techniques are linked to the kind of applications they are used in, the description of the investigation of these techniques and the design and fabrication of the corresponding tools is split in three parts. Each part belongs to a specific kind of application and describes in detail the appropriate subtasks of Task 2.1 and Task 2.2. Some additional tools and grippers are described in Chapter 4.5: Additional Subsystems, page 46.

In Chapter 3.2.1, techniques for cell manipulation and the design and fabrication of a suction gripper and a micro pipette array is presented. Chapter 3.2.1.2 describes the specification of a lens assembly operation as well as the development and fabrication of a suitable microgripper with force sensor. Manufacturing of an SEM-suitable gripper and solutions how to cope with adhesion forces are reported in Chapter 3.2.3.

3.2.1 Cell Handling

For the investigation of cell handling techniques (**Deliverable D202**) various cell-handling experiments had to be performed. The first task was to find a suitable cell species. As cells are rather different in size, shape and elasticity, it appeared to be useful to commit to one specific, but representative cell species for the investigation of handling techniques and for the final handling demonstration. The main demand for the choice of the cell species was that the cells can easily be obtained and cultivated. Further on there should be a relation of the final handling demonstration, the placement of cells on defined positions, to a useful future application.

The most interesting applications, like electrophysiological measurements or simultaneous injection of pharmaceutical liquids or genetic material, can be imagined for nerve cells. So IBMT exemplarily chose OLN-93 oligodendroglia cells from the rat brain. These cells have dimensions of about 20 μm , can easily be cultivated,

have a high proliferation rate and show a slightly adherent growth. To investigate the handling techniques and to find the appropriate manipulator for handling cells, mechanical grippers and different suction systems have been exploited.



Figure 6: Cell handling with a 21 μm pipette

The best handling results were achieved with pipettes with an inner tip diameter similar to the dimensions of the cells (21 μm). By a very cautious application of suction pressure the cell was sucked into the tip of the pipette without deformation (Figure 6c). In this position the cell could be easily transported, well protected against the forces of the liquid stream of the surrounding medium. Only the deposition of the cells at a defined position remained somehow difficult. As the cells had to be blown out with a sufficient liquid stream in order to avoid adherence to the tip of the pipette, the cells stopped their movement in some distance from the pipette tip. This distance had to be taken into account when putting down the cell.

Another advantage of a relatively large pipette diameter is, that the aperture cannot be obstructed so easily by cell fragments or other particles of the culture medium, so that – in contrast to the smaller pipette dimensions – the handling of more than one cell with the same pipette is possible.

The surface of the pipette should preferably be hydrophobic. The suction pressure (and with this the liquid flow) should be alternating and high for the detachment of the cell. The control system of the robot should be able to detect when the cell is detached and moves with increasing velocity towards the aperture of the pipette. Now the suction pressure should be reduced rapidly, and the liquid flow should be stopped exactly when the cell just has entered the tip of the pipette. An ideal pipette would have some kind of “mesh” inside, in a short distance from the pipette tip, to catch the arriving cell and prevent it from disappearing within the pipette. A very short pressure pulse, inducing a short period of high liquid flow, should perform the deposition of the cell. The cell should preferably be adhered to its target position by a suction hole or a hydrophilic coating of the target substrate. The detachment of strongly adherent cells or the separation of cells growing confluent can only be performed by biochemical methods. For the handling of biological cells a suction gripper had to be developed (**Deliverable D203**). This goal was reached in two ways: On the one hand a commercial glass pipette was adapted to the gripper ball of the Miniman robot to get a suction tool within a relatively short period of time. Simultaneously, micromachined pipettes, partly with special shapes, partly arranged in array configurations, were developed with regard to the handling techniques specified before.

As an additional extensive task, which had not been explicitly specified in the project programme, a miniaturised electro-fluidic suction system had to be developed in order to allow a robot operation in semi-automated mode. The challenge was that this electro-fluidic system had to be small enough to be carried by the Miniman robot in order to avoid long stiff tube connections; only some electrical connections could be tolerated.

3.2.1.1 Integration of a Glass Pipette into the Gripper Ball

A novel approach based on the idea to use a piezo-principle for the generation of extremely small liquid flows, a new suction mechanism based on a small piezo tube has been developed. This mechanism was completely integrated into the gripper ball. The construction of the piezo suction gripper is outlined in Figure 7.

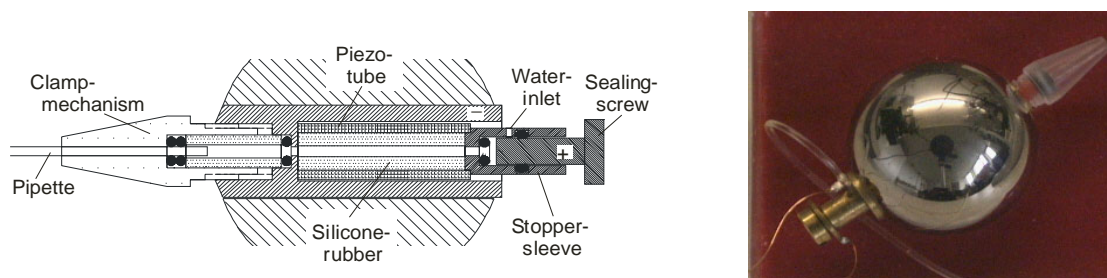


Figure 7: Construction drawing(left), Piezo suction gripper (right)

The clamp mechanism remained the same as before but additionally a piezo tube (supplied by Piezomechanik Dr. Lutz Pickelmann GmbH) is integrated within the gripper ball instead of the two-way-valve. The piezo tube has an inner diameter of 4 mm, a length of 18 mm and a wall thickness of 1 mm. Both the inner and the outer surface of the piezo tube are coated with a conductive ink. When a small voltage is applied between inner and outer surface of the tube it contracts in length and inner diameter, thus reducing its inner volume. In this way very small liquid volumes can be handled: The liquid volume which can be displaced by a defined voltage is equivalent to 327 pL/V.

For a reliable operation of the gripper there must not be any air in the suction system. Its high compressibility would lead to insufficient pressure due to the tiny contraction volume of the piezo.

To widely prevent the inclusion of air, the piezo tube was nearly completely filled with degassed silicone rubber, only a small channel was left right through the centre. The tube is closed by a specially designed stopper sleeve which allows the system to be completely filled with water and it can be hermetically sealed afterwards. The stopper sleeve further serves as an electrical connection to the inner electrode of the piezo cylinder. The electrical connection to the outer electrode of the piezo tube is made by the brass adapter. As a conductive connection material conductive silicone rubber was chosen. Its elasticity prevents the piezo tube from mechanical stress. The piezo tube is rigidly agglutinated only at its front ends, at the one side to the brass adapter, at the other side to the stopper sleeve. So the movements of the cylinder are only slightly restricted.

Before use, the system must be filled with filtered DI-water. For this purpose the sealing screw can be slightly unscrewed. The gripper is positioned with the pipette tip upturned and, bottom-up, slowly filled with water. After filling the volume can be sealed hermetically by the screw. The piezo suction gripper (Figure 7) needs no more silicone hose connection to the gripper ball and successful experiments showed convincing results.

3.2.1.2 Micro Pipette Array

A novel process for the production of micromachined pipettes has been developed. With this process transparent pipettes were produced, single or in an array arrangement of up to 3 x 3 pipettes at a distance of 150 μm . An overall view of a micromachined pipette can be seen in Figure 8.

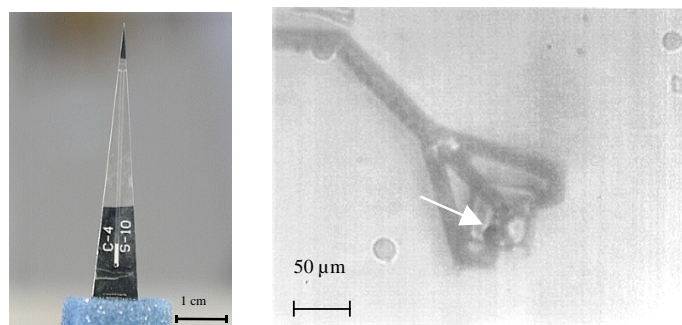


Figure 8: Micromachined pipette, overall view (left) and microscope image of nozzle and aspirated cell (right)

All pipettes consist of a liquid channel with a diameter of 10 μm , which meets a pyramidal transparent nozzle with a basis wedge length of 56 μm , a height of about 25 μm and an aperture of about 20 μm at its tip. The liquid channel of some pipettes splits into three channels before meeting the nozzle (Figure 8)

The liquid channels can be connected with the outside world via 500 μm drillings. A specially designed clamp adapter allows the connection of each liquid channel to thin flexible tubes. With a laboratory suction system cells could be sucked into the nozzle (Figure 8). They were transported under vision control within the nozzle and released again afterwards. IBMT has applied for a patent for the micro-pipettes as well as for its microfabrication process [Pat IBMT].

3.2.2 Handling of Mechanical Parts

3.2.2.1 Description of the Demonstrator Microsystem

In optical data storage, the data capacity is directly related to the spot-size of the focused laser. To increase the Numerical Aperture (NA) beyond that of the DVD system, a two-lens objective can be considered. The handling techniques required for such a system will be described in the following (**Deliverable D201**).

The assembly of two-lens objectives poses a new challenge, because the lenses are small and the alignment requirements are high. The typical decentering tolerance is 20 μm , while the tilt between the lenses should be less than 0.25 mrad. Furthermore, the lenses are coated, and should therefore be handled with great care.

For the Miniman demonstrator we have chosen to assemble a similar lens set consisting of two lenses and a mount. Miniman aims at small products. Therefore the lens size is reduced to the minimum diameters that are currently available, *i.e.* 1 mm (front lens) and 2 mm (main lens).



Figure 9: The Gel-Pak™ micro-parts container

The mount (\varnothing 2.3 mm) has three banana-shaped holes, so that the main lens flat surface can be seen.

Both the lenses and the mount are delivered in a so called Gel-Pak shown in Figure 9. The Gel-Pak can also house more lenses and mounts than needed for one assembly.

Testing the assembly of the lenses can be done in two ways:

1. Measurement of the optical quality of the lens set in a Twyman-Green interferometer. This will not be appropriate for Miniman, because it would require expensive measuring equipment, and the lenses have not been designed with optical specifications.
2. Direct measurement of the alignment errors between the two lenses.

The only important test for the Miniman system is the measurement of tilt between the two lenses. Tilt can be measured by counting the fringes of the interference between a mirror and the two flats on the lenses. This requires a simple optical set-up, as shown in Figure 10. A laser projects light onto a half-transparent mirroring surface and its reflection is projected onto a CCD-camera via a half-transparent beam splitter. Part of the light travels through the mirror and reflects on one of the lenses. This light will show interference with the mirror ray. Tilting the lens will result in stripes on the CCD-sensor. The width of one light stripe or one dark stripe (called fringe) is 0.25λ . For a red laser with λ equal to 650 nm, this is 167.5 nm. Given the diameter of the visible region, the tilt can be computed. The Front-lens in the picture would therefore have a tilt relative to the mirror of 2 mrad. A perfectly aligned lens would show one uniform intensity of light. The relative tilt between the two lenses should be less than 0.25 mrad, which is 1.5 fringe over 1 mm distance.

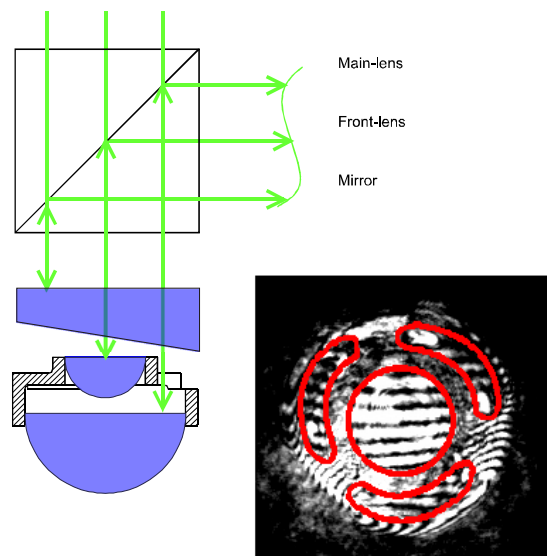


Figure 10: Lens Assembly and interferometrical patterns during adjustment

3.2.2.2 Development of the Micro Gripper

The design and the fabrication of the micro-tools have been addressed towards the fulfilment of the defined requirements in terms of size, assembly tolerances, and necessary grasping forces. Solutions devised in order to cope with adhesion forces during grasping of both biological and mechanical micro-objects have been implemented (such as a LIGA gripper with saw-like fingers) and are fully described in the previous reports. However, due to the size and the weight of the objects chosen by the user for the final demonstration, actually mini-lenses to be inserted and mutually aligned in a purposely devised frame, the adhesion forces are not relevant and do not give problems in the releasing phase. For the same reasons it would not have been a possible solution to improve the displacement amplification mechanism of the LIGA gripper in order to enhance the span and consequently the size of the objects which could be manipulated, as anticipated in the Technical Annex. Beside the necessary span, also weight and overall size of the lenses and the frame led to the choice of other fabrication technologies and materials in order to obtain more robust and reliable structures. The steps towards the chosen technology (Electro Discharge Machining - EDM), the material (Superelastic Alloy, Ni50.8Ti49.2) and the final gripper design have been previously described in the 2nd Progress Report. In Figure 11, a picture of the gripper (**Deliverable D204**) is shown.

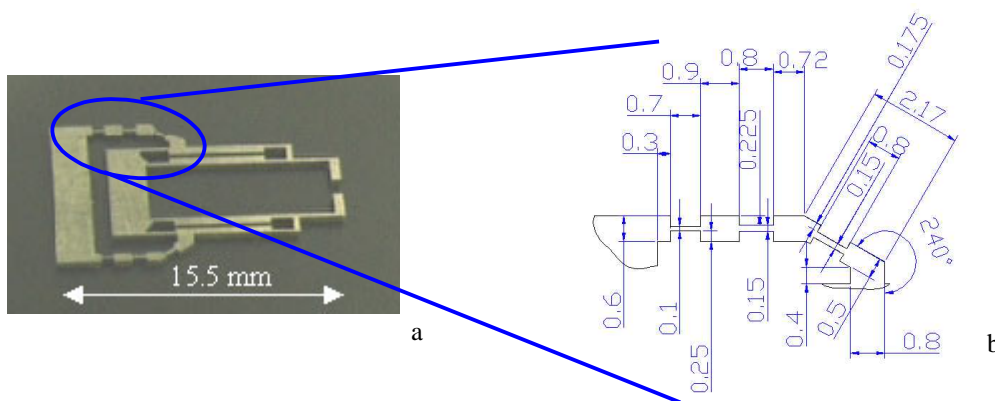


Figure 11: Superelastic alloy microgripper fabricated by EDM: (a) photograph of the prototype (dimensions: 15.5 mm × 8.4 mm × 0.5 mm); (b) flexure joints. The thinnest beam has a width of 100 μm and a length of 700 μm, and the smallest radius of curvature is ~0.055 mm.

EDM allows to fabricate high aspect-ratio structures made out of different conducting and semiconducting materials with good surface finishing and without any thermal alterations even in the smallest features. Moreover, even when the above characteristics are not strictly required (in our design the aspect ratio is ~5), EDM is a good choice to machine hard materials which could not be machined with other technologies. Superelastic alloy is the material of choice because of its favorable mechanical properties. When designing microstructures, rotary joints used in standard mechanics do not work efficiently and flexure joints often represent the preferred solution. Because of a limited displacement in the elastic range, each design of flexure joint microstructure is a trade-off between the need for large displacement and the requirement of minimum stress in material. For the intended micromanipulation applications we need a small volume microgripper with maximum span of ~2.5 mm, robust behavior and accurately controllable (e.g. piezoelectrically actuated). Superelastic alloy matches our requirements of span and robustness better than most other materials, e.g. stainless steel.

The microgripper was assembled in a suitably shaped housing fabricated in aluminium and brass according to the specifications of the assembly task, and characterised, Figure 12.



Figure 12: Gripper assembled in the symmetrical aluminum and brass mounting

During the development of the symmetrical gripper, several changes concerning the mechanical design have been taken. The latest design is shown in Figure 13 (left CAD-picture, right the final design)

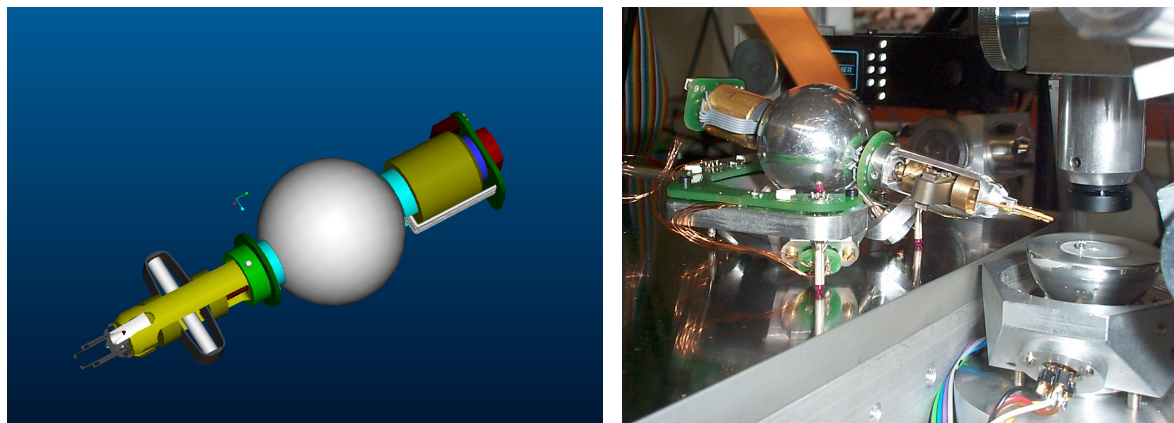


Figure 13: Re-designed gripper

In addition, a two-fingered gripper employing a scissors-like displacement amplification mechanism according to **Deliverable D206** has also been developed. This gripper principle has been abandoned, since it did not offer any advantages compared to the other grippers developed in the project.



Figure 14: Two-fingered gripper, driven by bimorphic piezoactuators

3.2.3 Handling Techniques inside the SEM

An exchangeable “Micro Tweezers” was developed, that serves several versions of Miniman as a gripper tool (**Deliverable D205**).

The principle (see Figure 15) is simple to explain: a cylinder 60 to 80 mm long is recessed in the centre portion with an indentation for a small multilayer piezo actuator that has 2 mm balls on both ends. One side of the piezo actuator rests on a set screw (“Pre-set gripper tension”), the other on the indentation milled in the end of the central recess (“pressure point”). The front end of the tweezers is undercut like a long bird’s beak, with a 4 mm hole where the undercut ends. This hole serves as a weak area in the cylinder, acting similar to a joint. The whole assembly is clamped in the manipulator sphere of Miniman III or at the carriage of Miniman IV’s manipulator. The counterweight that is required to balance the manipulator sphere is clamped to a 3 mm “Mounting cylinder”. It can be plugged into the gripper easily and provides a connector for the wires coming from the robot platform.

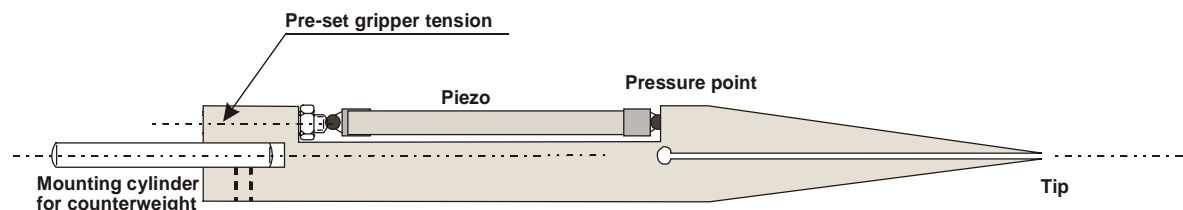


Figure 15: Working principle of the SEM gripper

The grasping operation was chosen asymmetrically, not analogue to the “thumb and forefinger” analogy you may expect: closing in on the particle from one side is easier to control (one degree of freedom instead of two that have to be synchronised). The gripper shown here is tilted 90° to the side. One side gently touches the particle that

must be grasped, and the other side closes in until the particle is caught safely. This avoids toppling or shifting of the particle - or loosing it completely in the worst case.

One of the most difficult tasks was the finishing of the fine front end (tip). For most experiments, it was decided to go through a manual fine grind and lapping process. This was done under a high quality stereo microscope, and it proved to be even more reliable than cutting a tip to size in a "Focused Ion Beam" (FIB) workstation. The only way to produce even better gripper tips is the use of micromachining techniques such as LIGA. However, these techniques are very expensive. Moreover, microsystems like such gripper tips require the development of adequate interfaces to the macro world. An approach basing on sub-grippers that can be grasped by larger micro grippers is a promising idea that will be evaluated in the future.

The extension of the piezo actuator is about 10 μm at 110 V, therefore the long leverage is needed. There is a distance of 3.5 mm from the weak (bending) point to the pressure point where the piezo rests off centre. Typically, the two halves of the "beak" are 30 to 40 mm long, forming a leverage ratio of 1:8.5, up to 1:11.5. The opening movement of the tweezers is therefore 85 to 115 μm . Some experiments were done with piezo actuators of longer stroke. However, their creeping characteristics were too strong. Therefore no more energy was put into this direction.

At present, particles of about 10 to 30 μm can be handled on a routine basis, 5 μm particles require good training. Therefore, the gripper shown here compares quite favourably with most other designs that go from millimetre to 100 μm size and fail with smaller objects.

3.3 Workpackage 3: Sensors

The sensors developed within this workpackage are employed in two ways. First, they provide the operator with feedback from the micro world and second, they provide position feedback for the control system.

To measure the extremely small forces in the micro world, force sensors based on strain-gauges have been designed and integrated into the microgrippers. A tactile sensor with 64 elements provides tactile feedback. It has been integrated into the tips of the 3-fingered gripper.

To enable Miniman to carry out tasks autonomously, a flexible, robust and integrated vision system has to be provided. This is realised with the use of an active vision-based system which provides positional and orientation information of tools and parts in the microrobot's field of operation. Furthermore, the sensor systems employed (light optical microscope and scanning electron microscope) have been enhanced by techniques to provide 3D-information.

3.3.1 Task 3.1: Force Sensors

For Miniman, strain gauges were selected for the implementation of force sensors, because of their small size, simple signal processing and adequate sensitivity. Actually, semiconductor strain gauges are available in sizes small enough to be mounted on the microgrippers. Processed from P-type silicon in orientations which provide maximum sensitivity to applied strain, they are available in both "bar" and "U" shaped configurations.

The integration of strain gauge sensors requires great care: when bonding semiconductor strain gauges, attention must be given to each process step as the quality of the finished assembly is totally dependent upon the correct process. The surface where the sensor has to be placed must be accurately cleaned, then a layer of strain gauge adhesive is applied and cured as a pre-coat. The glue layer is used also to obtain the electrical insulation of the sensor as regards the gripper body. The next stage in the bonding process is to abrade the cured pre-coat surface which generally possesses a glossy surface. A convenient way of achieving an ideal surface for the gluing process is to abrade the surface with pumice powder, previously moistened with neutraliser. The resulting surface is finally cleaned with conditioner and neutralised. Bonding the strain gauge is carried out by coating the (previously insulated) surface with glue where the gauge is to be bonded. The gauge is merely placed into position; no clamping is used as capillary action alone, between the gauge and the pre-coated surface, is sufficient to provide adhesion.

Finally, the gauge assembly must be cured following the manufacturers recommended cure schedules.

The process requires generally the maximum accuracy and experience; in our case, for the LIGA-fabricated microgrippers the task was even harder because of the pliability of the microgripper structure. Thus, the gripper was attached on a permanent magnet (nickel is rather magnetizable) to allow the operator to handle it easier; on the other hand, the magnetic field of the permanent magnet was not so strong to deform the gripper during the detachment.

The last delicate step consisted of the realisation of the electrical connections. Different solutions have been exploited for the different microgrippers according to the chosen strain gauges, Wheatstone bridge configuration

(one single sensor, two sensors, four sensors, depending on the gripper mechanical structure and size), and on the room available. In one case, two small metal points were soldered in the gripper body, and the two gold microwires coming from the strain gauge were welded to the two points. Finally, the electrical wires were joined to the metal points. In most cases the two gold microwires were directly connected to thicker wires.

In order to address the technical problems that must be solved to incorporate strain gauge force sensors in the microgripper, the starting point was a simple configuration based on just one single sensor glued in the position of maximum strain of a flexure joint of the microgripper. A bar-shaped semiconductor strain gauge was glued to the flexure joint at one side of the small version of the LIGA microgripper, as illustrated in Figure 16.

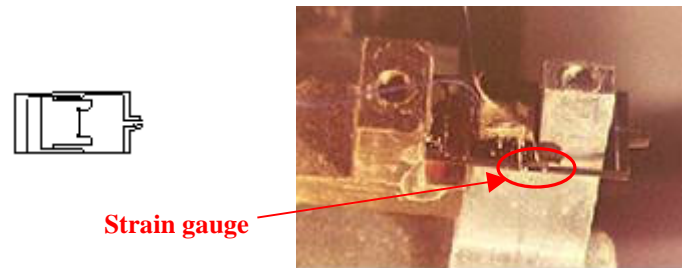


Figure 16: Small LIGA-fabricated microgripper and location of the single strain gauge

The Wheatstone bridge configuration was obtained by using three external precision resistors in the electronic circuit used for the signal conditioning.

The second step was, for the same model of microgripper, the integration of four U-shaped strain gauges. The optimal configuration would consist of a full Wheatstone bridge based on four active strain gauges. The four strain gauges should be mounted in two pairs, each located at a flexure joint: one strain gauge of the pair should measure compression and the other one should measure tension. However, in the case of our microgripper, it was physically impossible to glue strain gauges on the tensed sides of the joints, due to the small gap ($25\div 100\ \mu\text{m}$) between the two thin beams of each flexure joint. Therefore, it was decided to implement a (still) symmetrical strain gauge configuration consisting of a half Wheatstone bridge based on two active semiconductor strain gauges bonded to the compressed side of the two external beams of the gripper, and on two non active strain gauges. The location is shown in Figure 17.

After proper calibration, the output signal of the strain gauge can be read as a force signal. To this purpose, the strain gauge sensor was calibrated by opening the microgripper fingertip against a calibrated load cell (Model GM2 3M, PTC Electronics Inc., Wyckoff, NJ, USA - full scale 300 mN, accuracy 0.01 mN). Preliminary calibration tests showed the good linearity of the strain gauge sensor and indicated that the microstructural deformation of the microgripper can be monitored rather accurately using strain gauge sensors.

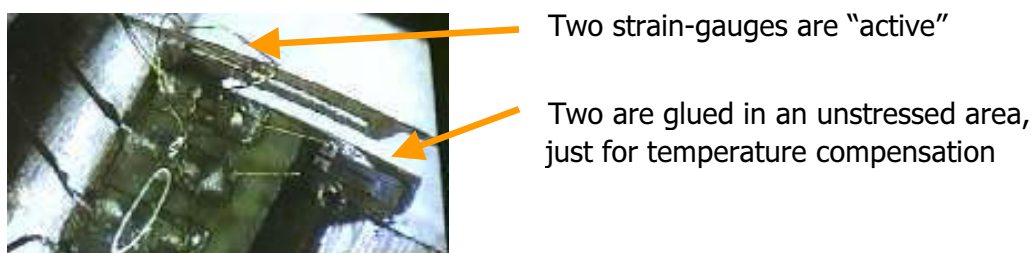


Figure 17: Small LIGA-fabricated microgripper: location of the four strain gauges.

With the sensors located in that position, when the gripper starts closing, the sensor output signal is related only to the finger position (*i.e.*, the strain gauge measures the finger deformation due to the external force generated just by the piezoelectric actuator). Then, as the fingertips touch the micro-object, the strain gauge measures a combined deformation due to both the external load and the actuator. Figure 18 shows the idling curve (solid line) and the curve obtained by grasping a micro-object (dashed line), and demonstrates that it is possible to identify and separate the signals related to force from the signal related to position.

The two curves are identical before the contact gripper-object (point A); therefore, the difference between the two curves gives the grasping force contribution (linear behaviour is assumed, and thus applicability of the principle of superposition of effects).

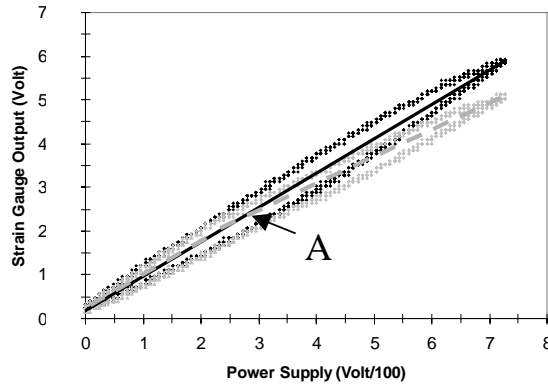


Figure 18: Strain gauge output signal vs. voltage supply to the piezo-actuator in idling (black curves) and in grasping (grey curves) conditions (optical fibre diameter = 190 µm)

With the big model of the LIGA microgripper the strain-gauge location has been changed in order not to have structure stress before contact with the grasped micro-object, and to have four active strain-gauges (Figure 19).

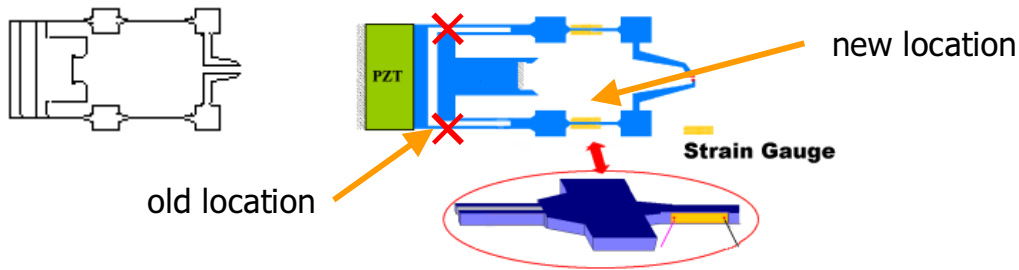


Figure 19: Big LIGA gripper: strain gauges location

As for the different models of LIGA-fabricated grippers, also for the EDM grippers commercial semiconductor strain-gauges have been used as force sensors. For the LIGA grippers different Wheatstone bridge configurations have been implemented, by using one, two or four active strain-gauges. As regards the EDM grippers, it was possible to use just two active strain-gauges because of the robustness of the mechanical structure of the gripper, which allowed to obtain a better noise ratio of the force signal compared to the one measured from the LIGA gripper. The force characterisation is illustrated in Figure 20.

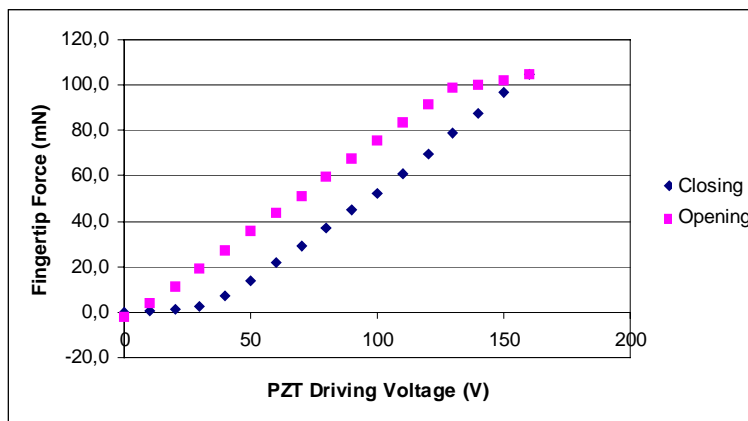


Figure 20: Force characterisation

For a better integration of the gripper within the Miniman system, different improvements concerning the gripper itself and the force sensors have been implemented. A thin gold layer has been sputtered onto the gripper in order to help the vision system during the automatic recognition of the gripper fingertips. The strain-gauge wires, seen by the vision system as undesired clutter, have been abutted to the fingers (see Figure 21, representing **Deliverable D301/D501**).

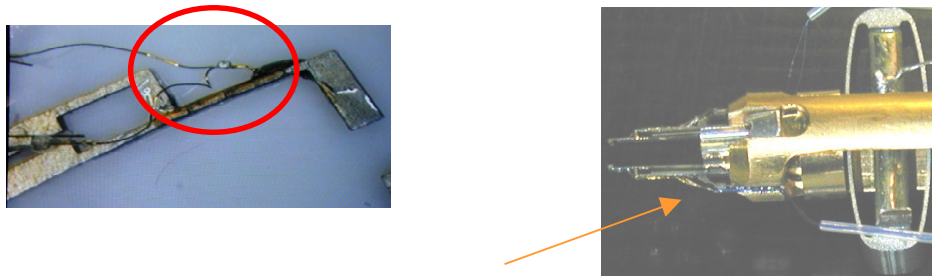


Figure 21: Strain-gauge wires: old (left) and new (right) configuration.

Moreover, the strain-gauge wires outside the Miniman sphere limited the gripper movements; this problem has been solved by placing them inside the sphere, in order to allow the orientation of the gripper. A printed circuit board for the gripper connecting wires (piezoactuator and sensor output) is mounted on the counterweight of the Miniman manipulator. It is also used for the LEDs of the global positioning system.

3.3.2 Task 3.2: Tactile Sensors

To allow touch detection during object handling, an IDT-based tactile sensor for a microrobot was developed. The sensor consists of two layers aligned to each other. One of them, the substrate layer, is structured with an array of paired thin film electrodes in an interdigital arrangement. The other layer consists of a film of insulating silicone rubber with an array of pyramidal elevations of conductive silicone rubber on its surface. If such a conductive pyramid is pressed against the corresponding pair of electrodes, the tip of the pyramid flattens and the resistance between the electrodes decreases with increasing pressure, because the ID-electrodes are increasingly short-circuited by the conductive silicone rubber.

As the available mounting space in a microgripper is very limited, and a wire bond connection of the sensor is not practicable for geometrical reasons, we decided to use polyimide foil as insulating substrate for the ID-electrodes as well as for the wiring of the sensor. As a minimum resolution to get a tactile impression of a simply shaped object, 8x8 pressure sensitive array elements have been used. To reduce the number of wire connections, the sensor should be addressed by row-column encoding.

The sensors were designed in two dimensions: One macroscopic sensor provided for test purposes is about 5 x 5 mm² of size. Each of its ID-electrodes has 26 fingers, which are 10 μm wide and have a distance of 10 μm from each other. The other one has a size of 0.9 x 0.9 mm². Each ID-electrode finger of the small sensor is only 5 μm wide, and also the distance of the fingers is 5 μm; with the available technology these dimensions were just as small as possible, and only 6 fingers for each ID-electrode could be placed. The latter sensor was planned for use with the microrobot.

The fabrication process comprises the microfabrication of the silicone rubber layer, the micromachining of the polyimide substrate with the ID-electrodes and the reliable alignment and connection of these both layers. The last step is the integration of the assembled tactile sensor in the gripper finger. The fabrication of the silicone rubber layer was accomplished by moulding a micromachined silicon mould. The silicon mould was produced by conventional KOH wet etch of a (110)-silicon wafer. With this anisotropic etch process, defined pyramid shaped holes can be obtained.

In the next step the holes are filled with a conductive silicone rubber material, then the wafer is covered by a layer of insulating silicone rubber. After curing the silicone rubber is removed from the mould. Figure 22 shows a photo of the resulting silicone layer. The silicone rubber material has been chosen with regard to optimal toughness and tensile strength. A liquid silicone rubber material supplied by WACKER was employed, which normally is used for keypad applications (ELASTOSIL® LR 3162 and ELASTOSIL® LR 3003).

An important task was to think about a suitable fixation of the silicone layer to the polyimide substrate. It has been accomplished by structuring a silicone frame surrounding the array of conductive silicone pyramids. For the mounting of the silicone layer onto the polyimide substrate, some silicone glue is applied to the outer contour of the frame. Then the two layers are aligned to each other by means of a flip-chip-bonder and slightly pressed together, until the glue is cured. The pressed frame protects the array against the penetration of glue, and the whole sensor is hermetically sealed afterwards.

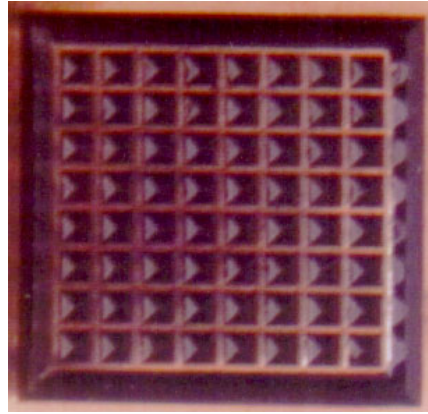


Figure 22: Structured silicone layer of the tactile sensor: Conductive silicone pyramids and a frame on a substrate of insulating silicone rubber

Owing to the provided row-column-encoding, the microfabrication of the polyimide substrate required the microstructuring of two metallic layers, which are insulated from each other with the exception of some through-connections: A silicon wafer is covered with a 5 µm polyimide layer. Then the first metallic layer with the ID-electrodes and conductor paths for the rows is structured on the polyimide. As electrode material a non-corroding material like gold was chosen in order to avoid later contacting problems, which could occur due to oxidation of the ID-electrode surface. Afterwards the ID-electrode area was covered by a chromium layer, which had to serve as an etch stop layer in a later process step. Then an insulating polyimide layer is applied and the via holes are structured with a dry etch process. The second metallic layer with the conductor paths for the columns and solder pads is structured on the polyimide and covered by a third polyimide layer. In a polyimide dry etch process, the sensors are separated and the solder pads are opened. In the same step the ID-electrode area is uncovered too, with the chromium film serving as an etch stop layer. The chromium is removed by a wet etch process afterwards, thereby the ID-electrodes are uncovered. The last step is the deposition of Ti-Cu-Ti-Au at the solder pads, then the polyimide foil with electrodes can be removed from the supporting wafer.

Because the removal of the chromium film turned out to be a problem, efforts were made to improve the process by replacing the chromium etch stop layer by other materials and by varying the electrode materials. With these measures the results could be clearly improved, but unfortunately none of the combinations yielded really perfect results: Either the layers did not adhere, got cracks or the etch stop layer could not be removed again after the polyimide etch step. Additionally, sometimes there were short circuits between insulated conductor paths crossing each other. These problems were made worse by the fact, that each device was relatively large, so that each structure had a defect anywhere.

All the experience made with the first process and design were exploited to optimise the final design of the tactile sensor. This was possible after the shape of the gripper, which should be used for tactile sensor integration, was known. The shape of the sensor was adapted to the shape of the gripper finger. The layout design was modified in a way, that the number and area of crossed conductor paths was minimised, the solder pad area, and with this the whole polyimide substrate, became smaller. Additionally, the micromachining process for the polyimide substrate was modified in order to eliminate the critical etch stop process step.

The new process can be seen from Figure 23:



Figure 23: Improved process for the microfabrication of polyimide substrate

This time the conductor paths were structured first, both the paths for the rows and for the columns. The ID-electrode-area and the solder pads were structured in the second metallic layer. After covering with polyimide, the sensor structures at first were separated by polyimide dry etch. The discrete ID-electrode fingers were

uncovered together with the solder pads subsequently. As this last process step is very critical with respect to underetching, optical endpoint detection was an important means to determine the exact etching time.

Finally some well working tactile sensors were assembled (Figure 24, Figure 25, **Deliverable D302**).

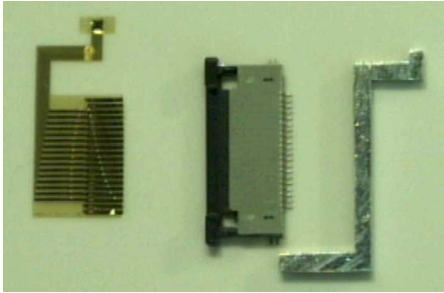


Figure 24: Complete tactile sensor with scheduled connector and finger of the Three Finger Gripper

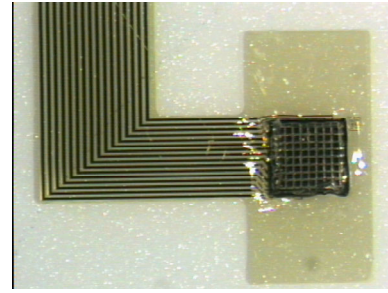


Figure 25: Sensor area of the tactile sensor

The scheduled clamp connector turned out to be too large and would damage the contact pads. Hence, the tactile sensors should be integrated without any clamp connector. It turned out, that the solder pads of the sensors detach very easily, making it impossible to solder the wires directly to the connector pads of the sensors. An adapter was conceived and glued to the sensor pads with conductive adhesive allowing the soldering of the wires (Figure 26).

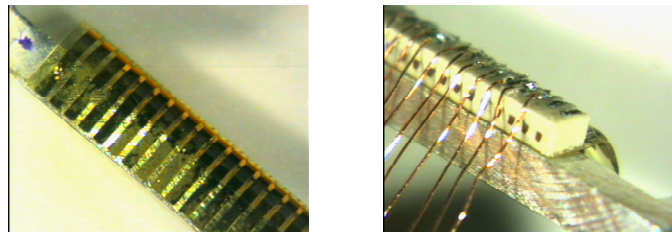


Figure 26: Connector sites of the tactile sensors, on the right after integration of the adapter

After complete integration, the performance of the originally well-working sensors had considerably deteriorated. Investigations revealed, that some of the interdigital electrodes had detached. The production of some new polyimide substrates with better adhesion of the metallic layers became necessary. After optimising the adhesiveness of the metallic layers, some better polyimide substrates have been produced. Now the wires were soldered directly to the solder pads of the polyimide substrate.

The next problem was, that, with the envisaged assembly technique, no flat glue connection could be achieved between the front area of the gripper finger and the tactile sensor, because the bend radius of the polyimide could not be made small enough. The problem was solved by removing the tip of the gripper finger and replacing it by a glass chip of equal thickness and suitable size. At first, the tactile sensor was glued to the flat glass chip, then the complete assembly was fixed at the gripper finger. In this way, some functioning tactile sensors has been successfully integrated in the gripper finger (Figure 27). This is **Deliverable D502**. The flexible design of the sensor allows an adaptation to other, even more complicated gripper shapes, too.

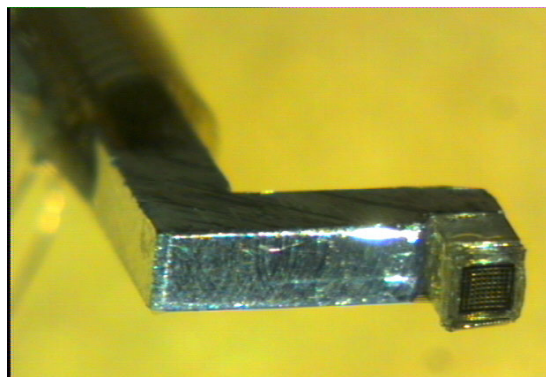


Figure 27: Tactile sensor integrated in one of the fingers of the Three Finger Gripper.

For the tactile sensor array a software-controlled sensor electronics was developed, which allows the readout of the resistance of the single array elements by row-column selection to minimise the number of wires – so for 64 tactile pixels only 16 connecting wires to the preprocessing hardware are necessary. A GAL addresses the rows successively with 5 V, while the remaining rows are driven to zero. For each row the voltages of all the columns are read out and represented graphically on a screen, fast enough to get a real time impression.

To calibrate the sensor, first the sensor response for each pixel is measured in unloaded condition. Then a glass chip is pressed on the sensor and the sensor response is measured in loaded condition. Assuming a linear sensor response, for each sensor element the individual offset and sensitivity is determined for correction of the measured values.

3.3.3 Task 3.3: Vision Sensors (Position Detection)

3.3.3.1 Vision sensor system (Deliverable D303)

The performance of an automated microrobot system depends to great extent on the performance of the system's sensors, which have to be able to provide the control system with accurate sensor signals in real time. To obtain a high performance of the sensor system, it was split into two parts: a global sensor and a local sensor. The global sensor system supervises the microrobot's work space to detect the position and orientation of the robot, whereas the actual operations by its manipulator are monitored with high accuracy by the local sensor system.

The global sensor is a high resolution CCD camera mounted to supervise the robot's work space. Local sensor is either an optical microscope with top-mounted camera, a CCD camera with macro objective or a scanning electron microscope with an additionally integrated miniature camera. For details about the different environments, please consult Chapters 4.2 to 4.4.

Global position sensor system

The robot is located by the global camera system with the help of four infrared LEDs mounted on top of the platform (cf. Chapter 3.1.1). Though three LEDs forming a non-equilateral triangle would be enough to detect position and orientation of the robot platform unambiguously, an additional LED guarantees redundancy in case the manipulator ball occludes one of the LEDs. From the 2D pixel coordinates of the LEDs, their corresponding 3D world coordinates can be calculated. This is due to the fact, that the z-coordinate of the LEDs is always known, either because the microscope provides the current z-position of the specimen stage or the stage has a fixed position - as in the case of the lens assembly station.

The vision system can distinguish between the different types of microrobots (Miniman III-1, Miniman III-2, Miniman IV) since each robot has a unique arrangement of LEDs. By calculating the distances between the LEDs and comparing them to the known actual distances, the robots can be identified unambiguously even if one LED is occluded. Calibration of the global camera is done using Tsai's 11 parameter camera model [Tsai 87].

In order to locate the robot globally, the LEDs in the image of the global camera have to be located. The LED spots were isolated from the rest of the scene by capturing two images, one with the LEDs turned on and another with the LEDs turned off. The absolute difference between these images only contains the LEDs. This difference image method is used only for determination of the initial position. Once the robot has been located the LEDs stay turned on and they are searched in the neighbourhood of their previous position.

All position calculations are done with sub-pixel accuracy. With the global position system the Miniman robot can be controlled with an accuracy of about 0.5 mm. This is sufficient to navigate to robot's manipulator into the field of view of the local sensor. Once the tool has reached the local sensor vision and controller make use of the higher resolution position data from the local sensor.

The global position sensor is not limited to only detect the platform position. It was extended for coarse position control of the manipulating unit. As the 3D coordinates of the centre of the manipulator sphere are provided by the LEDs mounted on the positioning unit, two more LEDs on the manipulator are sufficient to calculate the orientation of the manipulator. Both the SEM gripper (Chapter 3.2.3) and the EDM gripper (Chapter 3.2.2.2) are equipped with two LEDs at the counter weight of the manipulator.

Local sensor system

The local sensor system provides visual feedback from the working area of the manipulation-tool. Depending on the size and type of the objects to be handled, either an SEM (nanometre to micron range), a light optical microscope (micron to millimetre range) or a CCD camera with macro objective (millimetre range) is used for acquiring images.

3.3.3.2 2D Vision methods

In order to facilitate the development of the Miniman vision system, a software environment called Mimas was conceived. The Mimas package is developed in C++ with an extensible and well specified class hierarchy in order to ensure its continuous use beyond the Miniman project. It is embedded in the main system controller and plays an important role in providing the necessary information needed by the controller to locate and track all the moving parts to be handled as well as the micro-tools attached to the microrobot platform. Various imaging algorithms, vision techniques and other utilities have been integrated into Mimas in order to carry out the required demonstrations.

Object recognition

A number of different feature-based techniques for 2-D object recognition have been implemented within the vision system. Arbitrary shapes can be described and represented by selecting the appropriate features to extract from a scene. Object recognition strategies based on image features typically comprises two distinct stages. Firstly, features are extracted from the scene and, secondly, a search is performed to find groups of features that are consistent with the stored models in an object database.

Pairwise geometric histograms (PGH)

One of the three object recognition schemes implemented makes use of pairwise geometric histograms (PGH). PGH is a robust, statistically based method that allows scene image features to be classified according to known model features [Evans 93]. The method can handle both occlusion and clutter and is well suited to many 2-D recognition tasks.

When a scene image is acquired, PGHs are generated and are used to construct scene histograms. These are matched against the model histograms. Object classification is validated by finding consistent labelling within the scene image using a probabilistic generalised Hough transform. This stage also determines the location and orientation of one or more object models in the scene. Because the PGH algorithm is computationally expensive, it is only employed in specific situations within the context of micro-assembly where computational speed is not a binding factor.

Multi-resolution chamfer matching (MCM)

For recognition of lenses, as required in demonstration DEM1: Assembly of a Micro Lens System (see Chapter 4.2, page 38), the PGH technique is unsuitable, because of the light reflecting characteristics of the lenses. Thus, the models for the two lenses had features that changed dramatically with the lighting conditions and therefore could not ensure robust and reliable recognition performance. For these reasons, an alternative recognition method was implemented, based on the Chamfer matching technique [Barrow 77]. Edges extracted from the scene and from the object model are transformed into distance maps through a two-pass filter operation. In order to locate the object in the scene, the distance map of the object is correlated against the distance map of the scene. Due to the computing cost required during the correlation process, a multiresolution (pyramidal search) approach was implemented which offers a coarse-to-fine search strategy. The approach essentially reduces the resolution of an image edge map using an edge preserving method and the correlation is performed on the lower resolution. This step roughly locates the object, with the location subsequently refined at each higher resolution (see Figure 28).

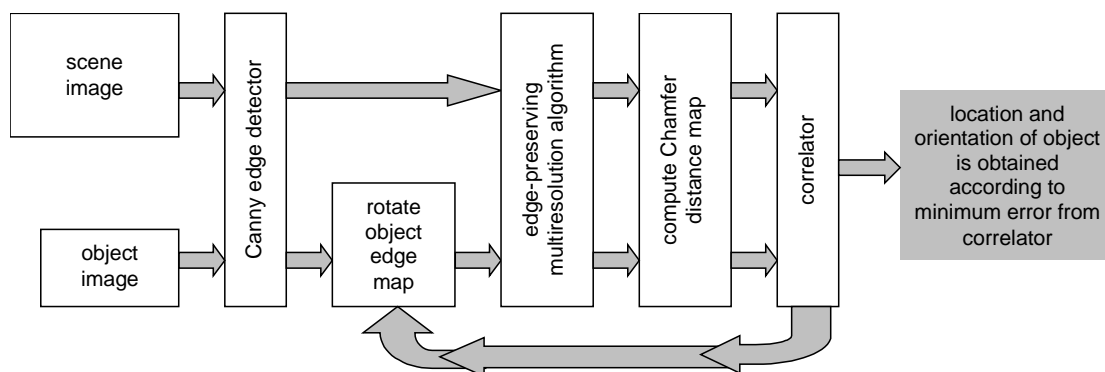


Figure 28: Strategy for multiresolution Chamfer matching.

It has been found that the MCM method is reliably suitable for locating both lenses. However, models of the objects to be recognised ought to be created only when the lighting conditions have been finalised since it was found that the method is not effective when a large change in shape/pattern (which is largely due to illumination changes) is observed.

Due to the fact that MCM is not invariant towards rotation, the template has to be rotated to a specified angle before a match is made. In practice, a range of angles is used for searching which further adds to the computational cost.

Active contours

In demonstration DEM3: Cell Handling (see Chapter 4.4, page 43), the main vision task is to recognise the boundaries of the cells, which have non-rigid shape. These characteristics make the PGH and the MCM methods unsuitable for the task. Hence, a third recognition scheme which uses active contours was implemented. An active contour (*snake*) is essentially an elastic closed-loop continuous curve that deforms and adapts itself to the shape of the object based on constraints placed by some chosen energy functions. One important advantage of using active contours is that it is fast and suitable for real-time operation, when properly optimised. Also prior knowledge of the boundary is not required, unlike rigid object recognition.

Figure 29 below shows an example of running the *greedy* algorithm on a typical image of cells in an aqueous solution taken from a camera mounted on an optical microscope.

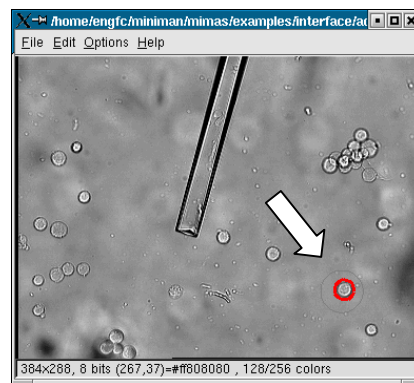


Figure 29: Typical result produced by the greedy snake algorithm (pointed by white arrow).

Tracking

The development of a real-time tracking algorithm for the control system has involved the analysis and trial implementation of various methods. It has been found that correlation based methods working directly on gray-level images were the most appropriate to meet the real-time performance requirements for the tasks. It was further found that when objects contain weak features, feature-based tracking methods often fail. For example, the Kanade-Lucas-Tomasi (KLT) tracker [Shi 94] was unable to track cells having weak features, while correlation methods were found to be successful.

In order to improve the performance of the tracking algorithm, an automatic template update scheme has been implemented which can work in two modalities. The first requires the tracking template to be updated repeatedly after a fixed number of frames. In the second mode, the template is updated only after the correlation value falls below a specified threshold - this removes the need for predicting a template update rate. When the correlation value drops below the threshold, one of the following situations may have occurred: (1) the lighting conditions on the scene have changed, (2) the background of the object template has changed or (3) the object has rotated slightly. Because of these factors, the application of the template update scheme is necessary in order to achieve accurate tracking. It is worth noting that the implementation is such that arbitrary polygonal shapes may be tracked, *i.e.* it is not limited to rectangular regions.

3.3.3.3 Depth estimation

The local sensor system as it had been described so far can only provide two-dimensional information about objects' locations and the tool position. However, for the automation of assembly tasks as the one presented in Chapter 4.2, page 38, depth information is essential.

Requirements made on a depth measurement system for Miniman are

- ease of integration into an existing local sensor system (*i.e.* SEM, light optical microscope and macro-camera)
- fast and robust depth measurement
- affordability in order to keep the costs of the Miniman system at a reasonable level
- the height accuracy should be at least in the range of the lateral accuracy of the local sensor system

Considering these requirements, triangulation based methods appear to be most suited. The following sections describe a triangulation method for gaining microscopic 3D information from an optical local sensor system. A similar, yet highly innovative method was also developed for the SEM.

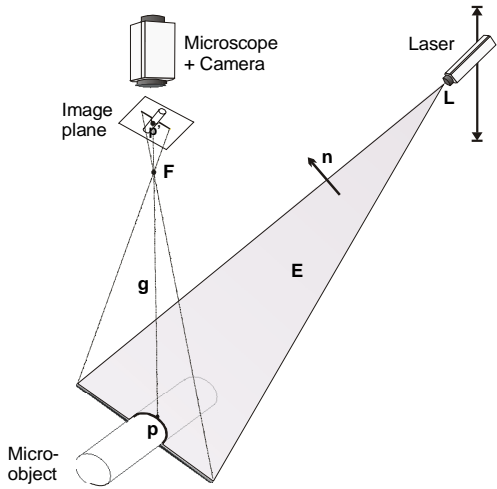


Figure 30: Sheet of light triangulation principle

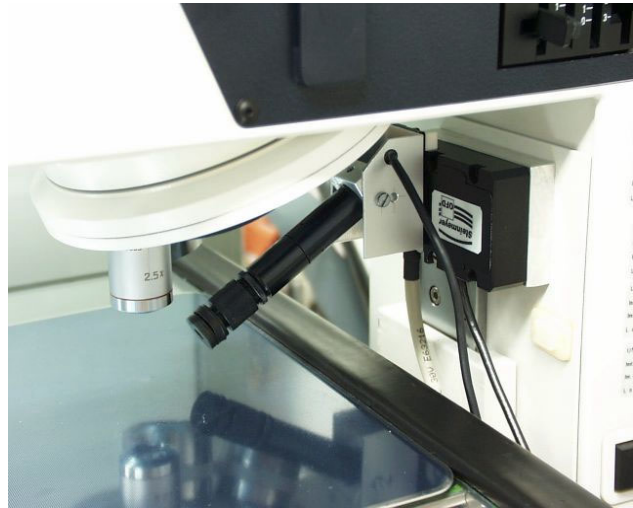


Figure 31: Laser depth measuring system integrated into the optical microscope

The measuring system consists of a line laser mounted on a micro positioning table which in turn is either fixed to the microscope housing (Figure 31) or mounted behind the macro-camera of the lens assembly station. The laser can be moved vertically in 100 nm steps allowing the laser line to be positioned on arbitrary objects in the scene. In the general *sheet of light* triangulation approach (Figure 30), the intersection of the laser sheet-of-light with the projection ray of the microscope image point to be measured is calculated. This requires the exact laser position and projection angle as well as the projection parameters of the optical sensor system formed by microscope and camera, to be known. Possible specification inaccuracies will be accumulated. The system developed within Miniman however makes use of the robot's planar working surface. The line projected on the ground floor serves as a reference line. An object in the range of the laser sheet generates a displacement of the line (see Figure 32). This offset directly corresponds to the object's height, described by the equation

$$\Delta h = \Delta y / \tan \varphi$$

where φ is the angle between the sheet of light and optical axis of the camera system. For instance, to measure the vertical alignment of the robot's gripper, a short horizontal segment of the laser line that lies on the gripper is chosen. Δy is the y-displacement between the chosen segment (herewith referred to as object line) and reference line. In contrast to the above mentioned general approach, the relative height Δh of an object only depends on two parameters, Δy and φ .

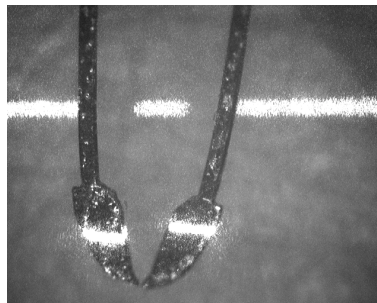


Figure 32: Displacement of the laser line corresponds to object height

Since a precise micro measuring table is used to position the laser, it is not necessary to have the reference and object line in view at once. The location of the reference line is determined only once, *i.e.* by storing a pair of parameters h_1 (laser table position) and y_1 (reference line position in the camera image).

Calibration of the system is performed in two steps: first, the scaling parameter of the optical system, *i.e.* microscope or macro-camera, is done as described on Page 21. Second, the angle between the laser sheet of light and optical axis of the camera system is calibrated automatically using the above equation for Δh after moving the laser table by Δh and determining the corresponding Δy . Several measurements are carried out and averaged. A fuzzy logic based image processing algorithm has been implemented to segment the line or line segments in the camera image. Standard segmentation methods proved unsuitable because they do not cope with the laser line's speckled boundary or pseudo line segments introduced by reflections.

Various experiments with different objects, *e.g.* grippers of different shape and material, coins and screws, showed that the measuring system is very robust. Fuzzy segmentation only fails at the occurrence of heavy reflections. This could be improved by automatic adaptation of the segmentation parameters. The measurement time (excluding image acquisition) varies from 10 to 40 μs . The accuracy that is reached with the described method depends on several factors. These are:

- the line segmentation accuracy (image processing)
- the local sensor system's magnification, *i.e.* the selected objective and the CCD camera's resolution
- the angle between sheet of light and camera axis

Assuming an angle of 45° between sheet of light and camera axis and a line segmentation accuracy of one pixel, the height resolution is equal to the lateral resolution.

One major advantage of the described sensor system is its flexibility. Resolution and size of effective range can be adjusted according to the application, *i.e.* the size of the micro objects and the necessary working area. Limitations are, as of all laser-based measuring principles, the dependency on the object's surface appearance. Dark and transparent materials are unsuitable.

To measure the co-ordinates of the manipulator's tool centre point (TCP), following steps are necessary: First, the 2D-coordinates of the manipulator are determined by object recognition. Using the 2D position information, the laser is positioned in such a way that the laser line intersects with the manipulator at an arbitrary location. Then the height of the intersection line is calculated as describe above. From this height, the z-co-ordinate of the TCP is derived, since now the plane in which the manipulator lies is fully determined by the intersection line and the position of the centre of the manipulator sphere. An additional feature of the depth recovery system is the possibility of measuring the complete profile of a scene.

3.3.3.4 Using vision feedback in the assembly of a micro-lens system (DEM1)

In demonstration DEM1, the vision system is required to recognise and track a number of objects. The order of operation is as follows:

1. recognise large lens using MCM
2. recognise small lens using MCM
3. recognise lens mount using PGH
4. recognise and track the two microgripper tips using PGH and correlation tracking

Two separate correlation trackers are used to track the microgripper models according to the tracking regions. The initial orientation of the region being tracked is provided by the PGH algorithm. However orientation of these regions cannot be updated since correlation does not return orientation information. This could cause the correlator to fail due to the large errors computed if the object is rotated by a significant angle. To prevent this condition, the template image is updated automatically using a specified threshold.

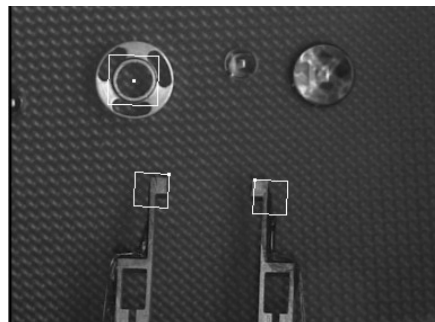


Figure 33: Recognition of the gripper pair and the lens mount using PGH.

Figure 33 shows the tracking region overlaid on the left and right microgrippers and the lens mount after all the objects have been recognised using PGH.

To recognise the lenses, the MCM method is employed. Figure 34 (i) and (ii) demonstrate the recognition ability of MCM in locating the small and large lenses, respectively.

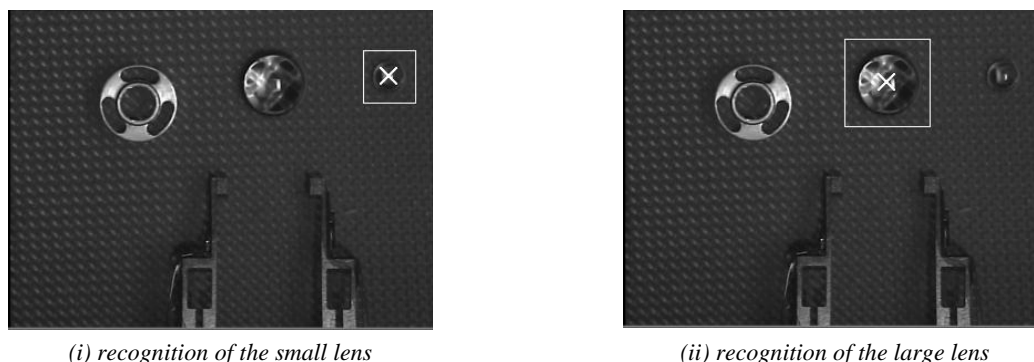


Figure 34: Recognition of lenses using MCM.

When PGH and MCM are applied to DEM1, the results are improved by the use of an initial region of interest around the object of interest. For example, if it can be assumed that the grippers are always in the bottom half of the frame at the beginning of the demonstration, then the recognition algorithm need not consider edges or lines in the upper part of the image. The same argument can be applied for the lens mount and both lenses if they, too, are located in a known region of the image. Selecting a region of interest improves the recognition results and speeds up the operation considerably. Furthermore, this is important because of the presence of unwanted edges or lines due to the highly textural background of the Gel-Pak used.

3.3.3.5 Using vision feedback in a cell handling task (DEM3)

In demonstration DEM3, the task consists of the transportation of user-selected cells in an aqueous solution using a micro-pipette operated by a suction mechanism. In this demonstration, the tasks are carried out in semi-autonomous mode. The vision system is expected to:

1. recognise and track a micro-pipette tip using a customised scheme (described below)
2. recognise and track cells using the active contours and the correlation tracking methods, with the aid of the operator

Due to the requirement that the micro-pipette tip may be completely occluded when the tip crosses an electrode on the electrode array, an ad-hoc method was designed for this task. Furthermore, the pipette tip does not contain enough distinct lines for techniques like PGH to be able to work efficiently and the correlation tracking algorithm generally fails on occluded objects.

The designed method makes use of the Haynes and Jain edge-change detector (HJEC) [Haynes 83] and an edge following routine which measures the depth of lines into the image. The second stage of the routine uses the edges from the HJEC method and measures the depth of lines into the image using a recursive search routine. The lines are sorted according to length and, based on a percentage threshold score, the longest lines derived from the micro-pipette are selected. The average value of these longest lines provides the y co-ordinate estimate of the micro-pipette tip, with the x values corresponding to each long line averaged to provide the estimated x co-ordinate of the micro-pipette tip.

One of the key features of the designed scheme is that it is able to hold the last detected position of the micro-pipette tip during operation. This allows successful tracking even when the pipette tip becomes occluded or even totally concealed during the crossing of the electrodes. In this situation, the method is able to self-recover when the pipette tip becomes visible again.

Figure 35 below shows the basic operations involved in the execution of this scheme.

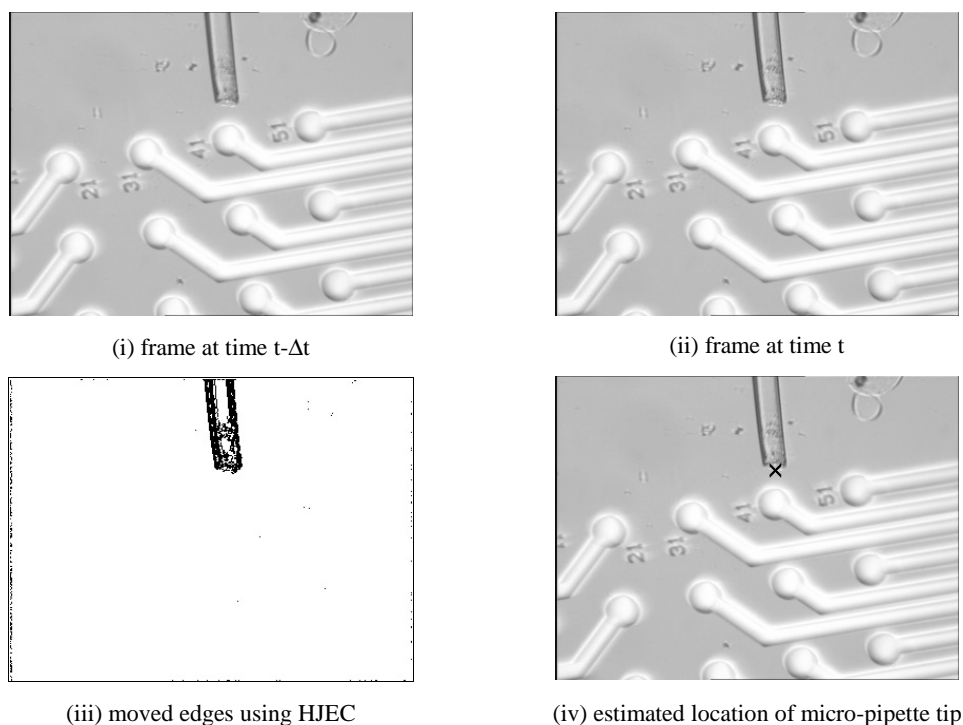


Figure 35: Operation of the customised method for pipette recognition/tracking applied to sequence (i) and (ii). The location of the pipette tip is determined by using an edge following algorithm on image (iii). The estimated tip of the pipette is shown in figure (iv).

The method described above has a dual purpose for both recognition and tracking. Due to the fact that only edges in motion are considered, in order to obtain an initial recognition of the micro-pipette tip, an image is first captured at time $t-\Delta t$, the pipette is then moved by a few micrometres and an image at time t is captured. The pair of images is fed into the method and the initial location of the pipette tip is found. The search time for subsequent images is reduced by constraining the search to a region of interest based on the last recognition/tracking result. In practice, it has been found that the algorithm takes no more than 110 ms (on a 1GHz Pentium III machine) to detect/track the micro-pipette when using an image resolution of 384×288 and hence is well suited for real time operation.

At the beginning of the cell handling task, the human operator is required to identify the approximate location of the cell of interest by a mouse click. An active contour, larger than the size of the cell, is then placed around the point selected and energy minimisation, as detailed in Chapter 3.3.3.2, is executed on the active contour to minimise it to the boundaries of the cell. The points of the polygon enveloping the cell are then sent to the correlation tracker which is used for tracking the cell while it is sucked into the micro-pipette.

An example of using an active contour is shown in Figure 36. If the cells are clustered then an optimal selection of the initial contour size is required, since if it is set too large it will detect the cluster instead of the cell of interest. This situation is shown in Figure 36 (ii) and (iii), respectively.

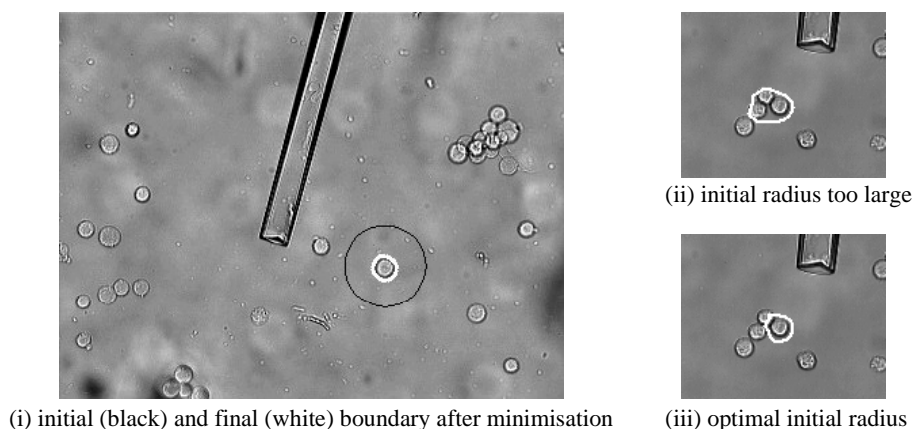


Figure 36: Determining cell boundary using active contours by a click-to-grasp approach.

3.3.4 Summary

Being one of many Miniman's achievements, the work accomplished in workpackage 3 has shown that it is possible to carry out typical industrial tasks in (semi-)autonomous mode using machine vision as the principal system feedback agent.

To provide information from the micro world both in automated and tele-manipulated mode of the Miniman system, a force sensor has been integrated into the two-fingered gripper. The three-fingered gripper was equipped with a tactile sensor. Vision feedback, which is essential for the control system, is delivered by a sensor system consisting of two parts: a global sensor for coarse position information and a local sensor for high resolution feedback from the micro operation area. The local sensor has been enhanced to provide 3D information. A major subject of this workpackage was the development of computer vision algorithms.

In the field of machine vision, porting generic solutions from academic research to an industrial application often introduces difficult challenges. For instance, solutions originating from academic research are often based on the assumption that the working environment is ideal, *e.g.* the quality of the acquired images is excellent, the objects of interest are always visible and not occluded and no clutter is ever present. In addition, external factors such as changes in the lighting conditions are generally ignored. However, when operating within an industrial application environment, these assumption are never held and a number of physical and other constraints often play a damaging role to reliable and robust system performance. In this case, generic solutions are rarely applicable and more ad-hoc alternatives are sought.

In particular, in the case of the lens assembly demonstration, the utilisation of a common industrial part such as the Gel-Pak, has introduced serious problems to the recognition of the other parts (gripper tips, lenses and lens mount) because of its textural appearance. Even by controlling and ensuring *similar* lighting conditions, it was found difficult to remove clutter generated by the Gel-Pak background (edge texture) without removing important features (edges) from the other objects recognisable in the given image. One way of solving the problem is to carefully tune a set of recognition parameters. This operation is generally required every time changes in external conditions and in the image acquisition apparatus occur (*e.g.* a different CCD camera being used).

As a corollary, it can be said that although autonomous operation through vision in an industrial task is certainly possible, its success and performance are still largely determined by the experience of the human expert.

In conclusion, it can be said, that it is not possible to build a versatile vision system, that can easily be adapted - by simply adjusting some parameters - to the variety of different applications the Miniman system is suitable for. Every vision problem is to a certain extent unique and requires a tailor-made solution. Furthermore, when real-time performance is required, the computational power of the current hardware is another limiting factor for the complexity of possible solutions.

3.4 Workpackage 4: Control System

The goal of this workpackage was to develop the control system that allows telemanipulation or semi-automation of the microrobots. The workpackage includes the design of both a software and a hardware part of the control system that has to ensure the microrobots' operation in real-time.

3.4.1 Task 4.1: Computer System

The Miniman computer system consists of two main parts: a central top-level control computer (a Dual Pentium III PC) and a hybrid parallel computer array performing low-level control tasks and signal generation. In this parallel multiprocessor system (PMS, **Deliverable D404**), the computer modules are placed on a backplane, which offers a high-bandwidth real-time communication channel consisting of dual-ported RAM modules offering a shared memory for a close processor linkage.

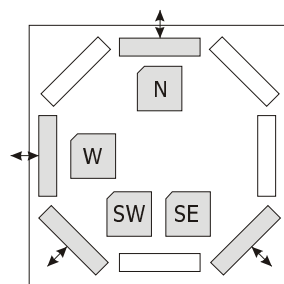


Figure 37: Schematic of the DPR backplane modules which can be connected to up to eight neighbouring modules. DPR modules are labelled according to the points of the compass.

Figure 37 shows a schematic of a backplane module on which either Pentium PC modules meeting the PC104 industry standard or Siemens C167 microcontroller modules can be placed. Each module can be connected to up to eight neighbours, where the layout ensures that every two computer modules are connected by one DPR chip.

The layout of the parallel computer can easily be changed, *e.g.* when an additional microrobot or another special piece of hardware is added to the system.

The PC modules are used for communication tasks, *e.g.* communication with the top-level control PC running the user interface. On these modules, a communications daemon process is running which passes user commands to a real-time module. As an operating system, Real-Time Linux has been chosen to have an inexpensive but widely used and supported solution at hand. The Siemens C167 modules acting as embedded controllers are running only the client software without an operating system and work in a “slave”-mode, awaiting commands via the fast DPR connection (which offers a real-time communication channel), and generate signals for actuators and station periphery as required. Since the PMS acts as a diskless client, the aforementioned top-level PC, which also hosts the user interface, acts as a server. This mapping of control tasks onto the available control hardware makes real-time operation of the micro robots possible. The top-level PC is a Dual-Pentium 3 machine with 2×1000 MHz processors and 0.5 GB RAM. This machine offers enough computing power to host the user interface, computer vision algorithms and closed-loop control tasks.

The complexity of a control system like the Miniman control is reflected in the number of connectors, wires and adaptors. This situation is made even worse by the fact that each of the different robot types (Miniman III and Miniman III-2, each with either a suction, an EDM or an SEM gripper, the lens alignment unit, Miniman IV) needs a tailored set of signals to drive the specific robot components or subsystems (like manipulation units consisting only of a linear axis, non-existing platform subsystems in the case of the lens-alignment unit *etc.*). Therefore, each robot type needs a different printed circuit board to collect the necessary signals which are fed into the robot connector (typically, a 50-60 line ribbon cable). Nevertheless, almost all hardware components are kept compatible with all robots and their tools. However, the high connection complexity and diversity makes hardware debugging extremely difficult.

This situation emphasises the importance of the reduction of cables leading to the robot, as in the Miniman V system. A standardised communication protocol combined with a bus-like connection system common to all robot types is crucial for a micro robot system with numerous connectors and wires with dimensions similar to the overall robot dimensions.

3.4.2 Task 4.2: Power Electronic Circuits (Deliverable D405)

A specific Smart Power Integrated Circuit was designed to drive properly a single piezo-leg of the small Miniman V. Taking into account the Miniman V structure (see also chapter 3.5.1.2), 4 power outputs were needed to control each piezo-leg. This smart driver has one digital input and 4 power outputs.

A commercially available 1.2 μm BDC technology (Bipolar, DMOS, CMOS) was used to design these specific Smart Power Integrated Circuits. Using this technology it was possible to integrate both power and control circuitry in the same substrate to define a Smart Piezoactuator Unit (SPU), see also chapter 3.5.1.2. Analogue and digital circuitry for serial interface was implemented using standard library cells. Power drivers had to be custom designed.

The specific piezoelectric materials used to build up the microrobot units can be modelled as capacitors with nominal capacitance value of 25 nF. Power drivers had to be designed taking into account some specifications:

1. bias piezoelectric materials with specific voltage signal waveforms with a maximum voltage of 50V
2. supply enough current to charge and discharge this equivalent capacitance
3. interface with a digital input coming from a digital multiplexed stage.

Taking into account these specifications, a full custom High Voltage Operational Amplifier (HVOA) has been designed using the HBIMOSF technology from MIETEC-ALCATEL. The driver architecture consists of a low-voltage digital-analogue converter (DAC) and an analogue buffer, from the analogue library provided by the foundry, and the full custom High Voltage Operational Amplifiers (HVOA). A buffer stage is needed to drive the HVOA's input due to DAC's poor driving capabilities.

The design of the HVOA is based on a classical cross-coupled differential input pair operational amplifier adapted to work under high voltage conditions. The use of this differential input amplifier instead of classical single common source stage has been considered in order to improve the driving capabilities of the amplifier. At the input stage a source follower has been included in order to increase the input voltage range in such a way to be able to work with input signals from 0 to 5 V (low-voltage inputs). An output stage based on a half bridge configuration has been implemented using high voltage transistors.

The microrobot system needs specific information related to: a label for every piezo-leg, the kind of desired movement (x direction, y direction or rotation), the type of voltage driving waveform (sinusoidal or trapezoidal) and the frequency. In order to send all this information, the system uses 3 wires: clock (Clk), control (C) and data (Din). All the information about the Smart Piezo Unit (SPU) name, the desired movement and the voltage signal waveform is sent through the Data Input wire.

The digital circuitry implemented is optimised for a global control strategy. The digital input receives always four voltage phases (shifted 0°, 90°, 180° and 270°) and with the information of SPU name and type of movement, the digital circuitry determines which voltage phase has to be delivered to each power output.

In some cases, a distributed control strategy can be more convenient. The digital input receives the four voltage signals that the driver has to deliver to each power output. In this case, these signals could be different in amplitude or offset. The digital circuitry implemented also works with this mode of operation.

Therefore, the digital circuitry is able to work in both global and distributed mode of operation. These modes were programmed and tested using the same IC as smart driver.

Taking into account that when high speed of movement is needed the accuracy is not a priority, the system works with a variable speed sending signal waveforms with variable frequencies. The limits are defined as follows:

- Maximum accuracy: 256 samples per period, 310 Hz and 4 mm/s
- Maximum speed: 64 samples per period, 1240 Hz and 1.6 cm/s

This maximum speed fulfils the initial speed specifications of some cm/s. The maximum accuracy satisfies the initial accuracy specifications of 10 nm approximately.

This full custom smart driver has been designed and implemented using the HBIMOS-F technology. The layout and a picture of this IC is presented in Figure 38.

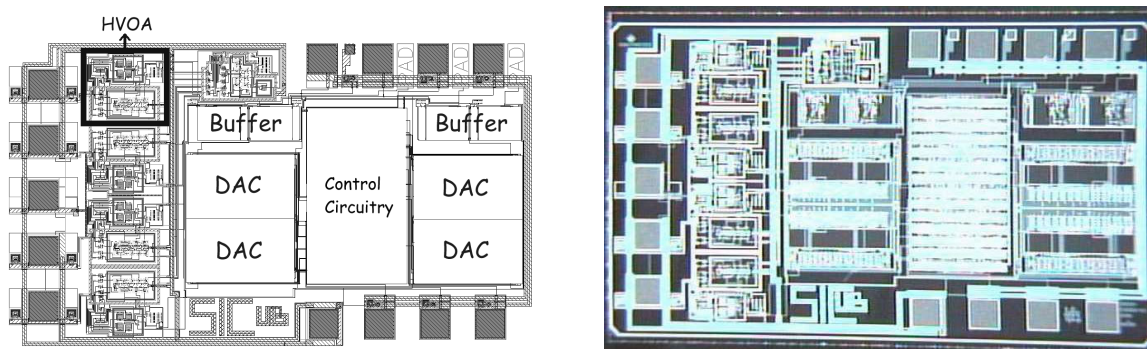


Figure 38: SPU Integrated circuit layout and its implementation

3.4.3 Task 4.3: Interface for Telemanipulation

For teleoperating the robot a 6D-Mouse is employed, that allows the user to use the microrobots in a very intuitive way (**Deliverable D401**). Additionally, both a graphical and a haptic interface for presenting the operator the force information acquired by the gripper was implemented.

3.4.3.1 6D-Mouse

A 6D-Mouse is a very intuitive and sensitive user interface, that is well known from other applications like navigating in a virtual reality or from using CAD-programs. It allows users to control up to 6 input parameters (X, Y, Z, roll, pitch, yaw) simultaneously. Movements in real 3D space are mapped by the 6D-Mouse to selectable axis of the robot. To allow an effective operation of the robot with the 6D-Mouse, the software has been steadily improved to match the experience made with the 6D-Mouse and the robot over the time.

Not only the activated axes are delivered by the 6D-Mouse, also the intensity of the user's input is available. This intensity is interpreted as a measure for the desired speed of the robot's movement in the corresponding axes. Since the robot can be used to act in several orders of magnitude, a "gear" change has been developed to maintain the sensitive and intuitive user interaction in any possible order of magnitude.



Figure 39: Axes of the 6D-Mouse (left); axes of the robot platform (X_p, Y_p, Z_p) and the manipulator sphere (X_s, Y_s, Z_s) (right)

3.4.3.2 Force Feedback

The gripper force feedback integrated into the Miniman system is based both on a graphical representation and a haptic interface, the commercial haptic interface “Phantom”. The specific characteristics which are necessary to use Phantom in micromanipulation tasks with the Miniman gripper are listed below:

- 1D constrain: the phantom tip position has to be constrained in only one dimension in order to convey an open/close operation of the gripper.
- Setting the force: an easy and intuitive way to set the force on the tip of the Phantom device.

This is done by a software purposely developed for the Miniman force feedback demonstrator.

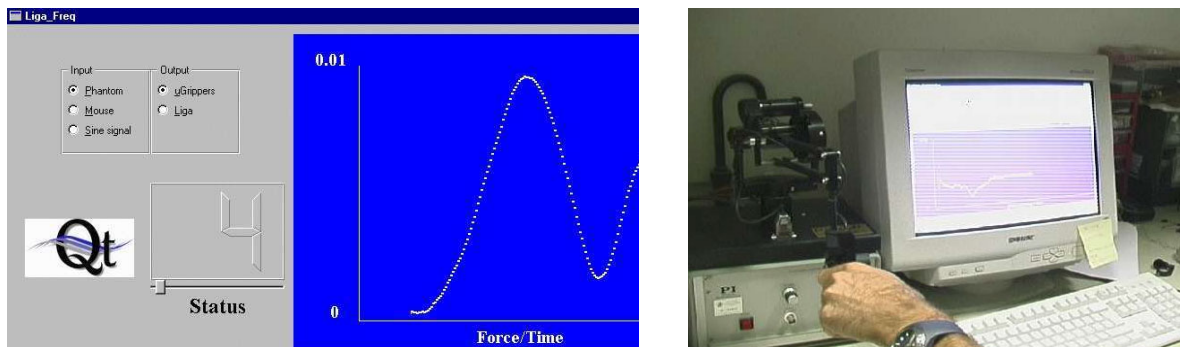


Figure 40: Qt graphical user interface (left), and Phantom haptic interface (right).

3.4.3.3 Hardware for signal amplification

The signals coming from and leading to the PC must be amplified by external hardware. This hardware is divided in two parts. It uses state-of-the-art electronic parts:

- one part of the hardware drives the piezo-actuator; this amplifier generates 0..150V out of 0..2.5V by using a PA42 high voltage amplifier from APEX
- the other part amplifies the signal coming from the strain gauges by using an AD524 from Analogue devices. The amplification factor of the AD524 is adjustable. The output voltage must range from 0..2.5V and is fed into the PC measurement card.

An integrated power supply unit generates +/-16V out from 220V~. An additional external power supply is used for providing +/- 150V for the high voltage amplifier.

3.4.4 Task 4.4: Control Algorithms

3.4.4.1 Design of the closed-loop controller (Deliverable D403)

The closed-loop control of the robots is based on the feedback information from the local and global sensor system (see Chapter 3.3.3.1, page 21). The global positioning provides the position of the robot's platform by

locating the platform LEDs. The coarse position of the manipulator is computed using the platform-position and a position of the sphere LEDs (as described on page 21).

The implemented closed-loop control algorithm works for all environments (light optical microscope, SEM and lens assembly station) and for all Miniman III and IV robots. There is also only one algorithm both for local and global control (*i.e.* coarse and fine motion) and also for control of both manipulator and platform. As the vision system is a passive system, the controller has to take care of getting all necessary position information. Images from the respective cameras are grabbed and passed to the vision system via IPC (cf. Chapter 3.5.2, Software Integration). Along with the images, the controller specifies, which position information it needs (*e.g.* position of gripper).

Though the implemented controller works quite well, it is not the optimal solution. The complexity of the problem imposes big difficulties on the controller design. However, a more advanced approach has not been pursued due to the lack of time which partially resulted from delays in the development of the vision system.

The quality of the closed-loop control system depends to a great extent on the accuracy, speed and reliability of the vision system. The flexibility of the Miniman robots is restricted by the flexibility of vision and control. For example, due to the low frequency of position updates from the vision system, the controller does not move the robot at maximum speed.

3.4.4.2 Force control

Force control of the EDM gripper that is utilised for the lens assembly (DEM1, see Chapter 4.2), is required for two reasons: First, the gripping force has to be limited in order not to damage the handled objects (especially the lens mount) or the gripper. Here, due to the immediate response of gripper and force sensor, the gripper is closed slowly while monitoring the force. As soon as the force reaches a specified threshold, the gripper voltage is held at the current value. The second use of force feedback is to detect slip, *i.e.* check if the gripped object is still gripped. This is done by evaluating the force from time to time.

3.4.5 Task 4.5: Environment for Semi-Automated Manipulation

An integrated environment for telemanipulated as well as sensor-based robot control has been implemented. This graphical user interface (GUI), called *ControlPanel* (Figure 41, **Deliverable D402**), not only allows to control different robots and grippers but also most parts of the sensor system and control hardware. This easy to use and yet powerful tool was written in C++ using the GUI toolkit Qt from Trolltech (www.trolltech.com).

Within the Miniman project, not only the power and flexibility of Qt was relevant, but also the multi-platform argument since not all partners of the consortium used Linux as development platform. With the help of Qt, for example the test programme for force measurement could be ported from Windows to Linux within minutes.

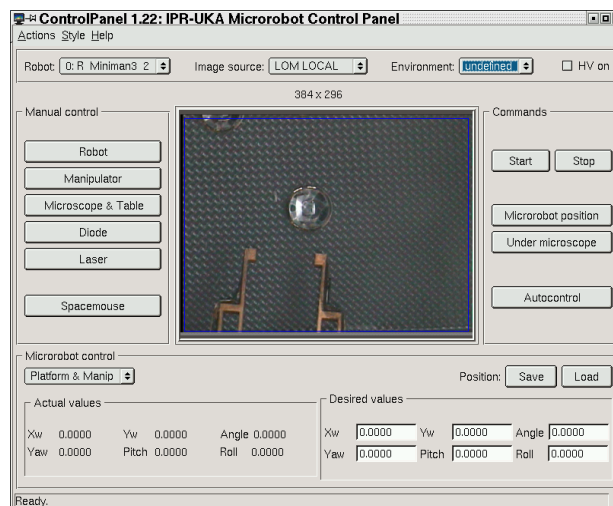


Figure 41: Main window of the integrated robot control GUI *ControlPanel*

3.5 Workpackage 5: System Integration and Demonstrations

The goal of this workpackage was the integration of all the components developed within the Miniman project into a microrobot system and the evaluation of the performance of the system by means of three demonstrations:

DEM1: Handling of micromechanical objects under a light microscope (see Chapter 4.2, page 38)

DEM2: Handling of micromechanical objects in a scanning electron microscope (see Chapter 4.3, page 42)

DEM3: Handling of biological objects under a light microscope (see Chapter 4.4, page 43)

These three demonstrations are performed by the Miniman III/IV system including an advanced sensor and control system. The fully miniaturised Miniman V robot is presented additionally to these demonstrations.

After the development of several single key components in the first project year, the partners integrated the hardware and software of the microrobots, their sensors and the control system. According to the reviewers' recommendations in the first review meeting, the Miniman consortium refined the technical details of the integration process starting from the exact specification of the three demonstrators. These quantitative functional requirements were transferred into the requirements on the robot subsystems and their interfaces, like that of the image processing unit, the computer system and the sensor integrated grippers.

The workpackage is divided into five tasks. One for the hardware integration, one for the software integration and one for each demonstrator. In this chapter, the methodologies of the integration work are discussed. This is done in detail only in case of the Miniman V system and the software integration. As the Miniman III/IV system's hardware consists of many subsystems, the integration issues are discussed in the respective chapters of the other workpackages. In order to avoid repetitions the realisation of the demonstrators is described in Chapter 4: Project achievements – Evaluation of Miniman.

3.5.1 Task 5.1: Hardware Integration

3.5.1.1 Miniman III/IV System

The integration work for the realisation of the Miniman III/IV hardware was structured according to the deliverables defined in the project programme.

- The design of Miniman III implies the integration of the micromanipulating unit in the micropositioning unit (**Deliverable D504**) by means of the manipulator sphere, which is described in Chapter 3.1.1, page 5.
- The manipulator sphere of Miniman III acts as the tool interface. Therefore, all micro tools had to be integrated in the sphere (**Deliverable D503**):

Integration of the micro pipette: see Chapter 3.2.1, p. 9

Microgripper for handling mechanical parts: see Chapter 3.2.1.2, p. 11

Integrated SEM gripper: see: Chapter 3.2.2.1, p. 11

- The integration of the force sensor (**D501**) and the tactile sensor (**D502**) in the micro grippers is described in Chapter 3.3.1, page 15, and Chapter 3.3.2, page 18, respectively.

Further integration work was required for the control system. The Miniman III/IV control system mainly consists of the parallel computer array that is described in Chapter 3.4.1, page 28. Additional circuits were needed for the connection of this computer system with the micro pipette and the lens gripper including the force sensors.

3.5.1.2 Miniman V System (D505)

One of the main objectives of the Miniman V development was the implementation of a microrobot with size as small as possible. The architecture of this microrobot has been defined full custom and very different from other more classical microrobots. The integration of the microelectronic driver with the mechanical piezoelectric structure, defining a Smart Piezoactuator Unit (SPU), is one of the key points.

Furthermore, different driving system strategies can be implemented by properly combining the SPUs. Specific interconnections had to be applied in order to implement a desired driving system strategy.

Finally, a demonstrator was implemented using a global control as a driving system strategy for the micropositioning unit and distributed control as a driving system strategy for the micromanipulation unit.

Smart Piezoactuator Unit

In order to define the best strategy for power signal distribution, we need to supply high voltage signals to the 24 contacts per microrobot-unit to define the desired type of movement.

CMOS standard integrated technologies are not capable to withstand this required biasing, so, usually, driver circuits for these piezoactuators are based on hybrid solutions using discrete components, like operational amplifiers, fabricated under non-available conditions. As a result of these hybrid solutions, the driver unit can not

be placed on the actuator unit. As a consequence, microrobot motion and precision performances are seriously limited by stress produced by the electrical link (more than 50 power wires in our case) between the actuator unit and the driver unit.

Using a BCD technology, a power driving circuitry with a proper interface control was designed to be integrated with the three-axial piezoelectric actuator defining the so called Smart Piezoactuator Unit (SPU). A full custom integrated circuit (IC) has been designed to properly drive one three-axial piezoceramic actuators element (piezo-leg).

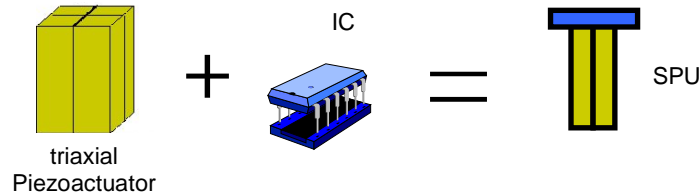


Figure 42: Smart Piezoactuator Unit concept (SPU).

For the Miniman V microrobot, 6 SPUs, are needed for micropositioning and micromanipulation units, as a consequence, 6 ICs have to be placed onto each platform.

In order to minimise the number of wires going to the microrobot, a serial interface protocol was defined. Furthermore, a Digital Signal Processor (DSP) is needed in order to read the serial interface protocol and properly distribute the data signal to each power output. This DSP device has been integrated in the same Integrated Circuit obtaining only one IC per SPU.

The microrobot needs some information in order to define a specific movement: the sort of movement, signal waveform and the desired speed. This information is sent in serial format and each Smart Piezoactuator Unit has to read it properly. Before sending this information, each SPU has to be labelled. The SPU name has to be sent in serial way connecting all the SPUs in cascade.

For Miniman V, two different driving system strategies were implemented in the Smart Power Integrated Circuit driver. This represents the **Deliverable D507** – Control algorithms for the piezoactuators of a microrobot with an integrated control module optimising the output signal of the power control electronics.

- A global control which applies four global voltage values to the four piezos of each leg and has the advantage to allow a higher speed. However, it results in a lower accuracy.
- A distributed control which allows to take the individual characteristics of each piezo into account by having the possibility to apply an individual voltage to each. This method has the advantage to allow a higher accuracy but will result in a lower speed.

System integration

The connections between the different blocks of the system are implemented using a printed circuit board (PCB). On this board, metallic connections and pads are printed in order to allow electrical connections between ICs, by means of a wire bonding technique. An epoxy material has been used for wire protection and heat sink. Connections between the 24 driver power outputs and piezoelectric actuators are performed by means of a flexible film.

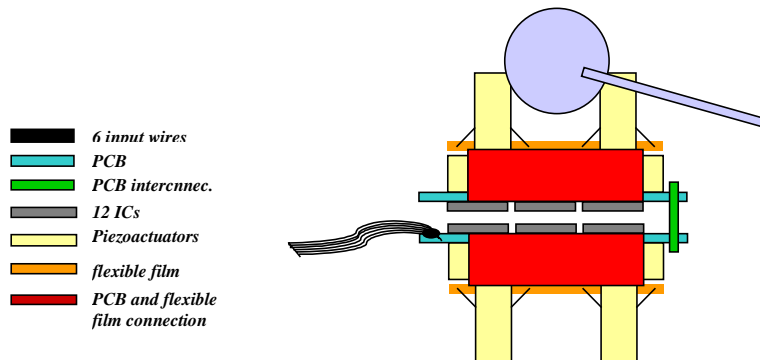


Figure 43: Microrobot platform assembling scheme

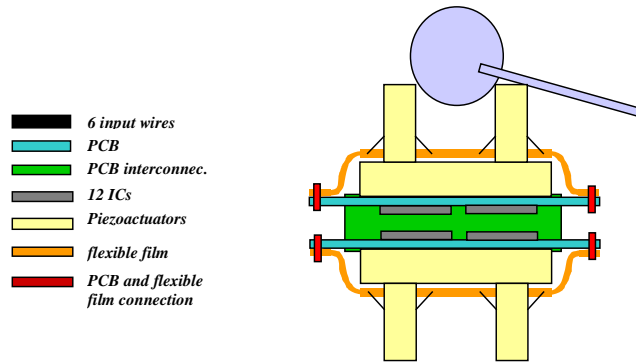


Figure 44: Microrobot platform assembling scheme rotated by 90°

Micropositioning and micromanipulation units are assembled identically. Power and digital wires arrive on the micropositioning unit from the control joystick module.

For the micropositioning unit assembling, global control strategy is used assembling 6 integrated circuits on a PCB board with the previously described routing. The 6 ICs on a PCB are called driving platform. A driving platform was implemented for the micropositioning unit using the global control strategy.

An epoxy layer was applied and this driving platform was assembled to the micropositioning unit using the flexible membrane.

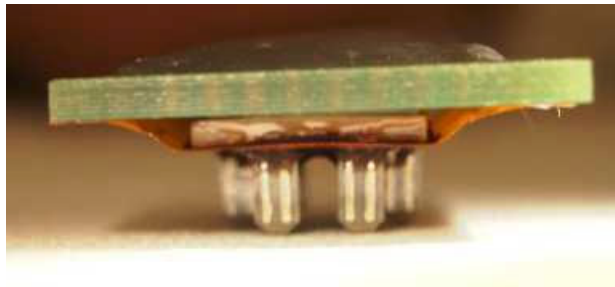


Figure 45: Final micropositioning unit assembly of Miniman V

A second driving platform was implemented for the micromanipulation unit using the distributed control strategy.

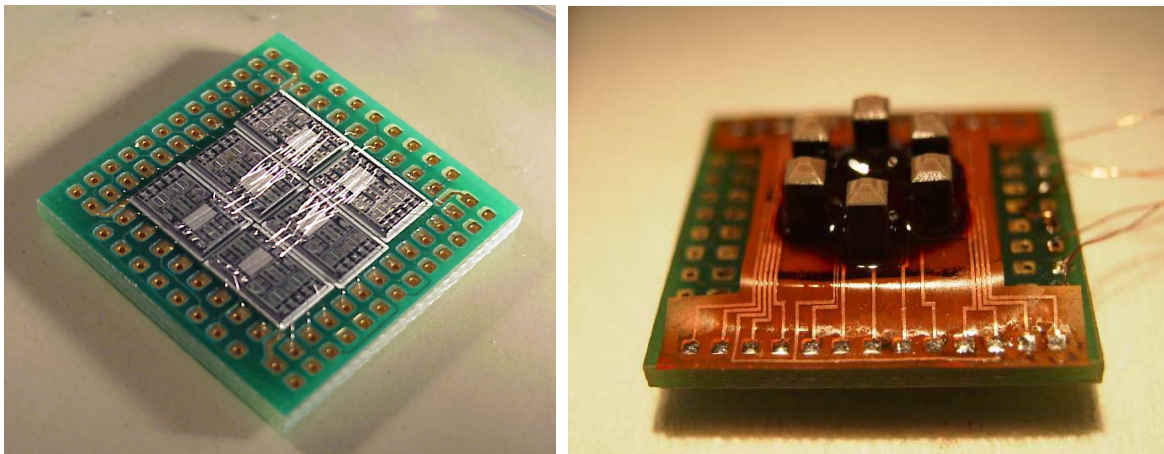


Figure 46: Picture of the driving platform interconnection for distributed control strategy used for micromanipulation unit and the final micromanipulation unit assembly of Miniman V

3.5.2 Task 5.2: Software Integration – Miniman III/IV System

As described in Chapter 3.4.1, page 28, the computer system for controlling the Miniman III/IV system consists of a parallel computer array and a Dual-1GHz Intel Pentium III PC. Being most important for the software integration, the architecture of the control system that is running on the PC is discussed in this chapter. As

described before, all software was programmed in C++. The GUI was built with the help of the graphical user interface toolkit Qt, which is also fully object oriented. The IDE “KDevelop” was used.

The realisation of the software corresponds to **Deliverable D508** – Control system with integrated pre-processing modules and GUI. Because of slight differences between the three demonstrator tasks, there are three versions of this structure implemented. All the classes can be divided into the groups sensors, control, user interfaces and communication. The central part is the control module that comprises the closed loop control. It communicates with the sensors on the one hand and with the so-called communication module on the other hand. The latter includes the interfaces for sending commands to the robots and the periphery of the system. Via Ethernet, the commands – *e.g.* for actuating the single piezo legs of the robots – are sent to the parallel computer system (which generates the signals for all electrodes).

The sensor module includes further interfaces that have been very important for the integration work. Its realisation corresponds to **Deliverable D506** – Control system with integrated pre-processing modules of sensors. There are two kinds of sensors used in the demonstrators – force and vision sensors. As the Miniman tactile sensor (see Chapter 4.5.2, page 46) was not required in these applications, it was not integrated in the software presented. Furthermore, there is a big difference between the pre-processing modules of the force sensors and the vision system. The pre-processing of the force sensor signals takes place mainly in the (hardware) circuits that are described in Chapter 3.4.3.3, page 31. The software integration of the force sensor is relatively simple (the IO-communication can be directly accessed by the assembly procedure programme). On the contrary, the integration of the vision system (being a complex piece of software itself) required a lot of co-ordination and integration work.

3.5.3 Demonstration Tasks 5.3, 5.4 and 5.5

As already mentioned, the realisation of the demonstrators is described in the following Chapter 4 “Project achievements – Evaluation of Miniman” in order to avoid repetitions.

4. Project achievements – Evaluation of Miniman

In this chapter, the results of the Miniman project are discussed. The evaluation of the Miniman project should show the novel approach solving problems in the minaturised world. This chapter corresponds with the **Deliverable DEV**.

Thinking about Miniman is thinking about flexible engineering. The flexibility makes it easy to do things like gripping parts, cell handling or acting in vacuum. Changing the tools of the robot (*i.e.* the gripper) changes the type of application without changing the robot. In order to illustrate how far Miniman can take this tasks, three different application had been chosen. These demonstrations are performed by the system around the Miniman III and Miniman IV robot prototypes. Beside these three demonstrations, the miniaturised prototype Miniman V is evaluated. Being in an early development stage and representing the future type of microrobots, this robot is not ready for being employed in real applications like its predecessors Miniman III and IV. However, its positioning and manipulating units are fully assembled and their performance is analysed. Finally, three additional Miniman developments are evaluated: a user interface for the feedback of micro forces, a tactile micro sensor and a micro pipette array. Being not required for the demonstrations they have not been fully integrated in the system yet. However, they prove the potential of the Miniman microrobots in further applications.

4.1 Miniaturised prototype Miniman V

According to the technical objectives stated at the beginning of the project a 5 DOF miniaturised robot with a size of a few cm³ driven by multilayer piezoactuators has been developed. It consists of a micropositioning unit and a micromanipulating unit, each made of a monolithic piezoceramic structure. In similarity to the Miniman III, the manipulating unit is adapted for the integration of a tool in the ball, but the tools developed for Miniman III are too voluminous and heavy to be a serious alternative. The first prototype is instead carrying a tungsten probe. Driving the stator units with the on-board high voltage integrated circuits and a quasistatic walking mechanism a motion resolution of 10 nm is possible and the maximum operation speed is 2 mm/s and 20°/s for the micropositioning unit and the micromanipulating unit respectively. The original specification was an operation speed of at least 3 cm/s and 45°/s and a motion resolution of 10 nm, but this was eased in the revised programme plan for the benefit of onboard ICs permitting a great reduction of the number of connecting wires. Using external power sources and waveform generators and inertial driving mechanisms an operation speed of several cm/s is expected.

A fabrication process for the monolithic multilayer miniaturised actuators has been developed. Taking the exploitation potential into consideration a wet building process is used. The technique has been pushed towards the limits to allow for the high degree of miniaturisation. Milling in the green ceramic state offers a versatile and cost-effective way of shaping tailor-made multilayer piezoceramic actuators, like the monolithic stator units in Miniman V. The specifications of Miniman V related to the electronics driving system are:

- Power electronics on board
- Serial interface protocol to minimise the number of wires to 6
- External portable power module
- Control module with different driving system strategies:
 1. Global control: expected speed of movement is around some mm/s and the accuracy is conditioned to technological parameters reliability (capacitance load values dispersion and height adjustment)
 2. Distributed control: lower speed of movement and accuracy in the range of 10 nm independent of technological parameters reliability. The electronics is able to make mechanical corrections.

The piezoceramic element tip movements are confined to a rhombic area. Within this area, the element tip can move arbitrarily depending on the waveform of the drive voltages. Various trajectories can be chosen. Figure 47 illustrates in two dimensions how the element tip moves for some suitable driving mechanisms. A trapezoidal or a sinusoidal waveform resulting in rhombic and elliptic trajectories is suitable for the walking mechanism. The rhombic trajectory has some apparent advantages. A longer vertical distance can be used for driving, the tangential velocity of the leg tip will be constant during each step (there are two steps in each drive cycle) and the step height will be maximised. On the other hand it might be possible that unwanted mechanical resonances are triggered. The waveform for inertial driving has to be adjusted so that the element tips manage to release from the ball at the uppermost position.

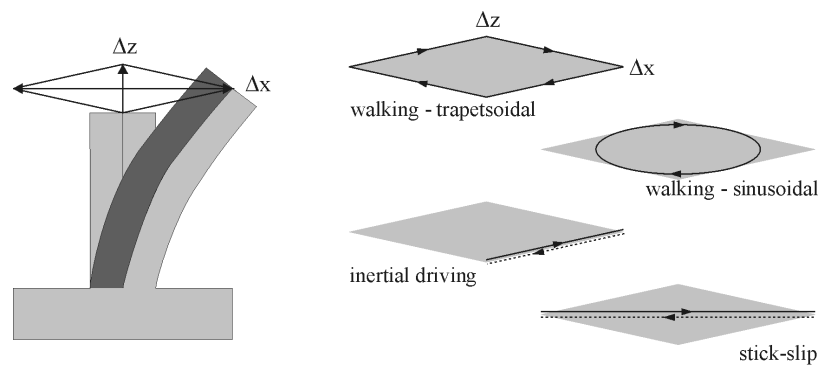


Figure 47: Illustration of the trajectory of the element tip for different types of waveforms. Possible tip locations are within the shaded area.

An experimental set-up with a precision gauge block made of hardened steel placed on a stator unit soldered via a flexible printed circuit to an IC socket was used to evaluate the performance. Displacements were measured with a length gauge system.

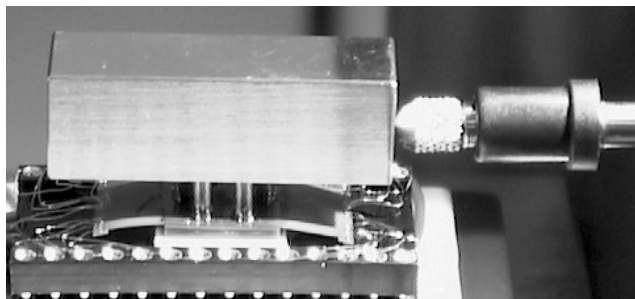


Figure 48: Experimental set-up for testing of the micropositioning unit. The stator unit is soldered to a flexible printed circuit, as in the microrobot, and an IC socket is used to connect to external electronics.

Inertial driving and walking motion with trapezoidal and sinusoidal waveforms have been tested. There was a difference in the step length with motion direction throughout all measurements. There are several possible explanations for this, but one of the most plausible reasons is lack of symmetry in the tip movements. A distortion of the rhombic area confining the possible locations for the tip is expected. Capacitance measurements have given values from 9 to 16 nF for different quadrants in the legs, indicating a large difference in active volume.

Another important fact is that the contact with the counter-surface sometimes takes place at the edge of the tip, not in the centre. Since the distortion and also the height and shape of the tip surface are not identical, the tip movement of all legs does not become uniform.

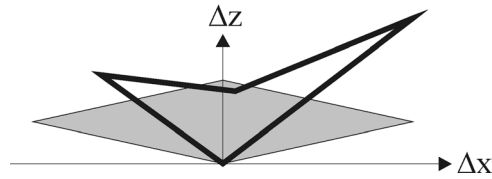


Figure 49: The rhombic area, which confines the possible locations for the element tip is distorted due to asymmetrical deflection of the drive element and possible contact with the counter surface at the edges of the drive element instead of the centre. The effect of the edge contact is strongly exaggerated in the figure. Ideal area is shaded.

A sinusoidal waveform gives the same step length as for the trapetsoidal waveform, which was not expected since a shorter vertical distance is used for driving. However, the elliptic trajectory gives less distortion than the rhombic trajectory and a greater part of the ideal drive length can be used. Inertial driving should give only half the step length compared to driving with rhombic waveform, but the step length is closer to the theoretical. This mechanism should be less sensitive to distortions and non-symmetries.

First tests have been made to drive a steel ball with the micromanipulating unit. Using the same experimental set-up, the steel ball could rotate in any of the three directions using a trapetsoidal waveform in the frequency range 500 Hz – 19 kHz. The peripheral speed was several cm/s at the highest frequency. The drive mechanism is believed to be some type of impact or inertial mechanism rather than walking. No post-processing had been done to the preshaped contacting surfaces, which made the spacing/fit between legs and ball too large in comparison with the step height. The micromanipulating unit was also tested preliminarily with a hybrid PCB prototype of the IC power drivers and a joystick control module. The ball could be turned in all three directions in the frequency range 220 Hz – 880 Hz.

The results from the first tests gave rise to a slight change in design. The tip geometry has been changed to accomplish a more accurate walking. The width of the elements has been increased and the design of the internal electrode pattern has been changed. Thereby, the maximum elongation has been increased from 1.1 μm to 1.3 μm and the capacitance level is more homogenous.

Tests with the new stator units differ from the results with the former actuator units. As expected, the trapetsoidal waveform gives longer step length than the sinusoidal waveform. Still, inertial driving and stick-slip gives less scatter in step length than the walking mechanisms. The unsatisfactorily spacing/fitting between the legs and the counter-surface makes it difficult to make a fair comparison between mechanisms. The large height deviations of the legs are connected to the level of miniaturisation and the complex electrode pattern chosen to get as high flexibility as possible.

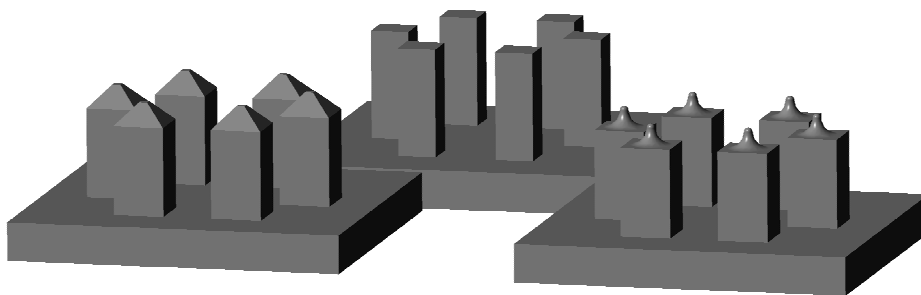


Figure 50: Improved geometry of the stator units. The micropositioning unit has a robust pyramidal tip and the micromanipulating unit has a sharper tip to make the contact with the ball favourable.

It can be concluded that a higher alignment accuracy is needed in order to achieve an improved position control using walking mechanisms and with actuator structures of this type.

4.2 DEM1: Assembly of a Micro Lens System

The demonstrator DEM1 shows the assembling of a micro lens system under a light optical microscope. The task is specified as follows (Figure 51).

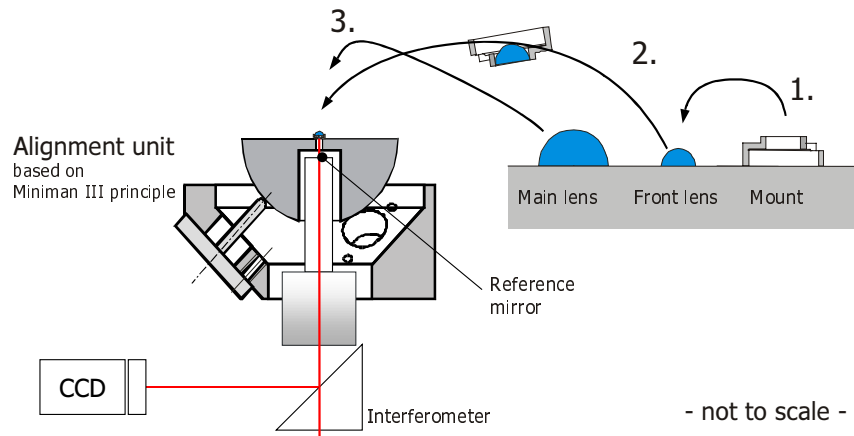


Figure 51: Lens assembly procedure

The robot Miniman III – equipped with an EDM superelastic alloy two fingered gripper – lifts the lens mount from the Gel-Pak, turns the mount by 180° and inserts the small front lens by releasing the mount atop the lens. Afterwards, the resulting front lens subassembly is lifted from the Gel-Pak and moved to the lens alignment unit (LAU). This unit consists of a laser interferometer, a modified Miniman III manipulation unit (hemisphere) and a reference mirror. Now, the robot grasps the main lens and coarse positions it in the subassembly. After aligning the reference mirror relatively to the main lens, the actual alignment of the lens system is performed by tilting the front lens subassembly relatively to the reference mirror by means of the lens alignment unit while checking the resulting interference patterns of the laser interferometer.

The lens assembly station (LAS) is a complete demonstration station to assemble small microoptical devices. The design and construction of this station is part of Workpackage 5.

To guide the operator through the demonstration procedure, a graphical user interface has been implemented. It provides a step by step guidance through the demonstration. For each step a description and the state of this step is displayed. If a step fails, the operator has the possibility to repeat a step, perform the step manually or activate one of the fallback solutions for the specific step. For example if the recognition of the gripper, the mount or the lenses fails, the operator can provide this positions of the objects by hand. To position the robot by himself the operator has the full power of the interface for teleoperation available, as described in Chapter 3.4.3, page 30.

4.2.1 The Gel-Pak

The assembly procedure starts at the Gel-Pak (see Figure 52). Here the initial step is to grasp the mount and rotate it by 180° (see also Figure 51). For this, Miniman is automatically moved by the global positioning from its arbitrary starting point to the working position in front of the Gel-Pak. After this, the gripper tips can be recognised by the Gel-Pak camera.

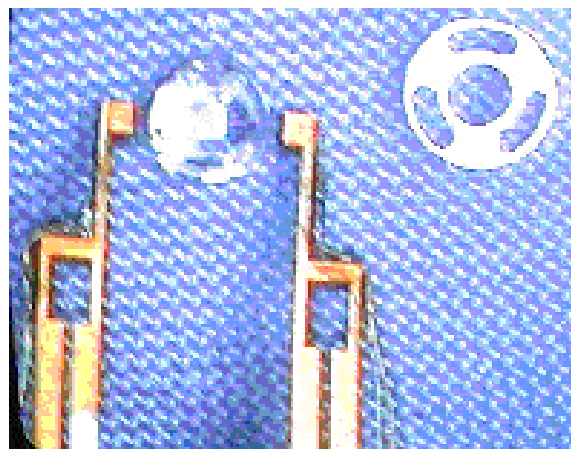
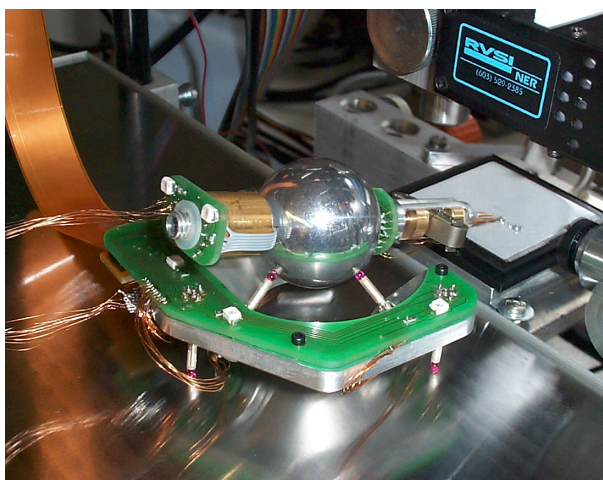


Figure 52: Miniman at the Gel-Pak

Now the vision-system starts moving the grippers close to the mount using the laser triangulation system. When this is done, the gripper will close to grip the mount. If the mount has been touched and the gripper tips begin closing, the force feedback loop starts, until the incoming signal from the strain gauges exceeds a specified value – when this happens, the control system knows that the mount has been safely gripped. At this point, the global positioning starts turning the mount by 180° automatically, and drops it down onto the Gel-Pak. The reason for dropping the mount is that Miniman does not provide an additional rotatory axis in its gripper, and with the mounting angle resulting from the 180° turn, it is impossible to place the mount over the small lens.

Now, the next step of the assembly procedure can be started. Miniman grips the mount again, this time with the correct assembly angle. The mount will now be put over the small lens. This is the first critical situation: due to the friction that keeps the small lens in the mount when Miniman will lift this subassembly, the orientation of the small lens in the mount is not fully determined (because there is no rim to completely align the lens during this procedure).

If the two parts (mount and lens) are in their correct tolerances, the insertion of the small lens will work perfect. At this point, assembly step 1 of Figure 51 is done.

4.2.2 Transferring the subassembly to the LAU

The next step is to transfer the small lens-mount subassembly to the LAU. This is performed by the global positioning system. At that point, the operator takes over manual control over Miniman to correctly position the subassembly into the recess of the LAU which accommodates the subassembly (refer to Figure 53).



Figure 53: The mount subassembly at the LAU

Once the subassembly is placed correctly in the LAU, part three of the assembly procedure can be started.

4.2.3 Mounting the main lens

After successfully placing the subassembly in the LAU, the next phase of the assembly procedure can be initiated. For this, the robot moves to the Gel-Pak again using the global positioning system and approaches the lens using the local positioning. The grasping process is monitored using the force information of the force sensors. When the control system can assume a safe grip, the Gel-Pak is set to release mode by applying vacuum. When lifting the lens from the Gel-Pak, a possible slipping condition is detected by monitoring the grasping force. If the force rapidly drops, the grippers have slipped and the lens has not been grasped.



Figure 54: Picking up the main lens from the Gel-Pak

Once the lens is grasped (see Figure 54), Miniman moves to the LAU again controlled by global positioning.

As soon as the main lens arrives at the LAU, control is again transferred to the user (Figure 55). Now the most important phase of the assembly procedure can be started: mounting and adjusting the main lens.

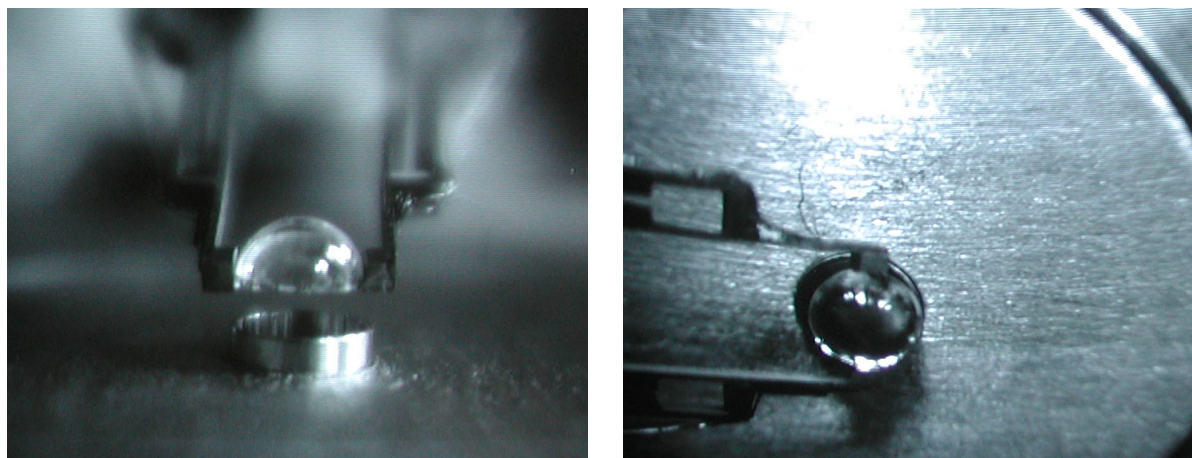


Figure 55: The main lens at the LAU held by Miniman

4.2.4 Alignment of the lens system

The final step is the alignment procedure. To initialise the measuring system (*i.e.* the laser interferometer), the operator has to align the reference mirror to the main lens first. This is done using the two micrometers of the LAU. The alignment itself is performed using two main controls:

- The roll axis of Miniman's gripper, handled with the space mouse
- The LAU's rotational axes

The interferometer camera is the output of the system, where the user can observe the interferometer patterns. Both, Miniman and LAU axes are controlled by the 6D-Mouse.

During the adjustment, the patterns visible on the monitor of the interferometer camera will change. In the interference pattern, the banana-shaped holes of the mount will give an interference pattern of the main lens while in the centre of the interference pattern, the small lens is visible. By changing the alignment of the two systems (Miniman and the LAU), both patterns can be optimised to show as few fringes as possible. With the system, it is possible to eliminate all fringes in the pattern, thereby reaching an alignment precision of 0.25 mrad as specified in Chapter 3.2.2.1, page 11 (see Figure 56).

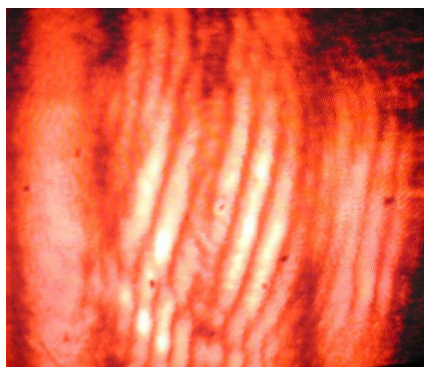


Figure 56: Interferometric pattern while adjusting the reference mirror

4.2.5 Results

A universal robotic system suitable for many tasks that is adapted to and applied for a single specific task cannot compete with a system that is specially tailored to this one particular task. This is true for commercially available robot systems which have to be adapted to the given application by a team of engineers or special system suppliers. This is still valid in the case of a micro robotic system, where several problems are worsened by problems specific to the micro world. This disproportion between the two approaches is also true when looking at risk, cost and throughput time, which are the commercially most important aspects.

When looking at a research environment and new technical frontiers, it is important to develop new systems. Especially if one considers the current situation, in which the lack of assembly facilities seems to obstruct the creation of new, highly innovative micro systems. In that framework, the Miniman robot is a highly interesting tool.

In the previous paragraphs it was explained that it is not justified to see the Miniman robot as a multi-functional robot, ready for fulfilling all kind of objectives. In the end, there is always something that needs to be changed to the concept, for fulfilling that specialised objective. Miniman's strength is to manipulate with a very large stroke (being the size of the base the robot works on) with a very small motion resolution. At the moment, the Miniman system is not suitable for fully automated assembly purposes, like the lens-assembly. The aspect of the Miniman system which is the closest to being a product which might be sold is the teleoperation of a pair of tweezers on several orders of magnitude.

These positive aspects do make the robot very suitable for working in a SEM, for example for wafer inspection in a laboratory (one or two assembly tasks in a row) environment. For industrial purposes (serial or mass production) its large stroke is too slow, which is –in this perspective– a negative aspect of the concept.

4.3 DEM2: Handling Tasks inside the SEM

According to the project programme, the aim of this demonstration task was the preparation, implementation and evaluation of a demonstrator to prove the Miniman system's capability for (partial) assembly of several highly miniaturised test products within the vacuum chamber of an SEM.

The final SEM demonstrator that was chosen by the Miniman Consortium is an example taken from the investigation of environmental pollution. Thanks to the advice received from researchers at University of Basel, Switzerland, some understanding was gained about the need for a manipulation system like Miniman. Figure 57 shows 10 µm dried down acid rain crystals on a damaged leaf. It would be very interesting for biologists to grasp these particles and carry them to a defined surface that is suitable for examining them by x-ray analysis.

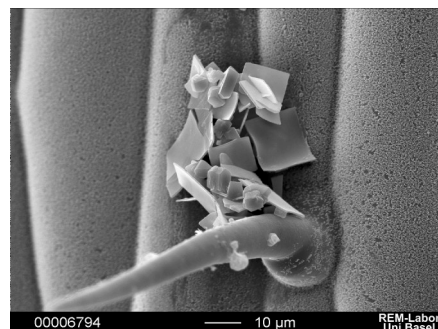


Figure 57: Acid crystals dried-down on a leaf.

Similar to the cell handling demonstration, this is an experiment the Miniman system is predestined for. In addition to the high resolution it requires the high flexibility and the intuitive teleoperation possibilities the Miniman system provides.

However, if microscopic objects of this size are to be handled, the so-called scaling effects must be faced very often. The most frequent effect caused by these unfamiliar force ratios is that a grasped object remains sticking at one jaw of the microgripper when trying to drop it. Furthermore, the particles observed with the help of the electron beam can be charged electrically – unless a so-called “Environmental SEM” working at elevated pressure is used. This makes manipulations unpredictable if no suitable actions are taken to cope with these problems. As proposed by [Miyazaki 97], one possible approach is to involve a second robot which is equipped with a “helping hand” consisting of a simple needle-shaped gripper tip. It can brush off the object, minimising the contact faces by the small dimensions of the needle.

Accordingly, Miniman III-1 is equipped with an SEM micro gripper to grasp the particles while Miniman IV acts as the helping hand. Its gripper can clamp very small probes that can easily be disposed when worn or dirty (see Figure 58).

To make these experiments possible, the SEM was modified as already described in Chapter 3.1.1, page 5. The small CCD camera described in Chapter 3.3.3.1, page 21, provides a lateral view that is very helpful during teleoperation. Although an automatic control basing on the developed vision and triangulation methods has not yet been integrated, the SEM demonstration shows an important result of the Miniman project. It was clearly shown, that particles as small as 10 to 30 µm could be retrieved by a mobile micro robot, and settled on pre-

determined locations. Especially in this demonstration, the 6D-mouse control (Chapter 3.4.3.1, page 30) with its “gear change” turned out to be the best suited user interface for this type of microrobots.

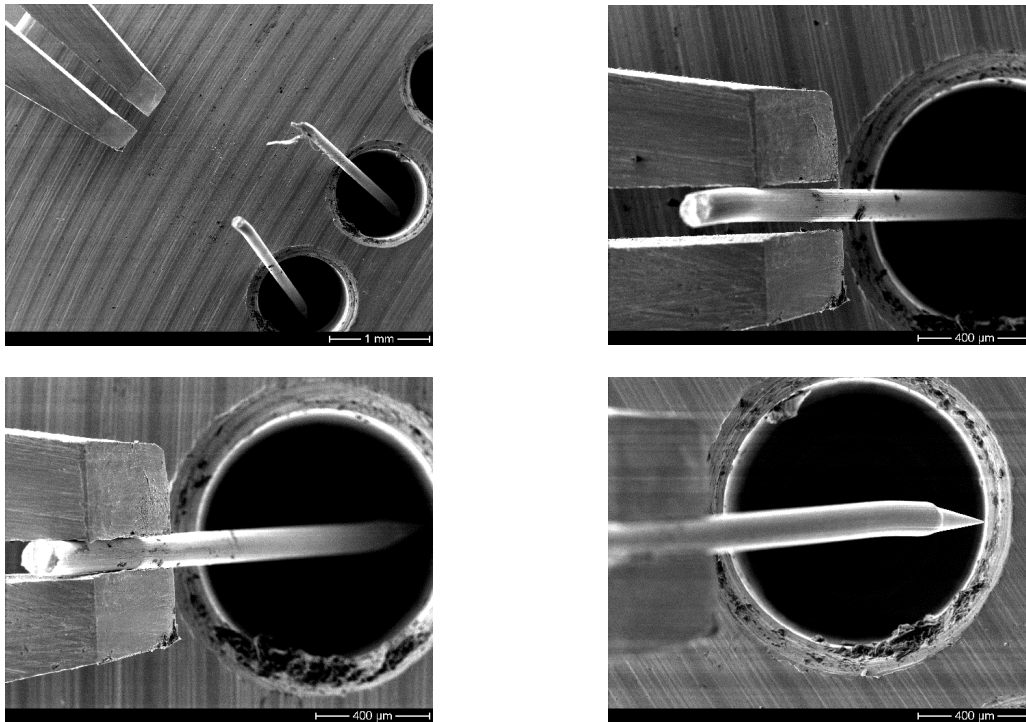


Figure 58: Miniman IV grasping a probe out of a repository (hole diameter 1 mm)

A further example demonstrating the grasping and releasing of a sphere, probably an incineration aerosol, with a diameter of only 15 μm is shown in Figure 59. It was taken from an ivy leaf. As one can see the sphere sticks at the opened gripper and has to be brushed off with the help of Miniman IV acting as helping hand.

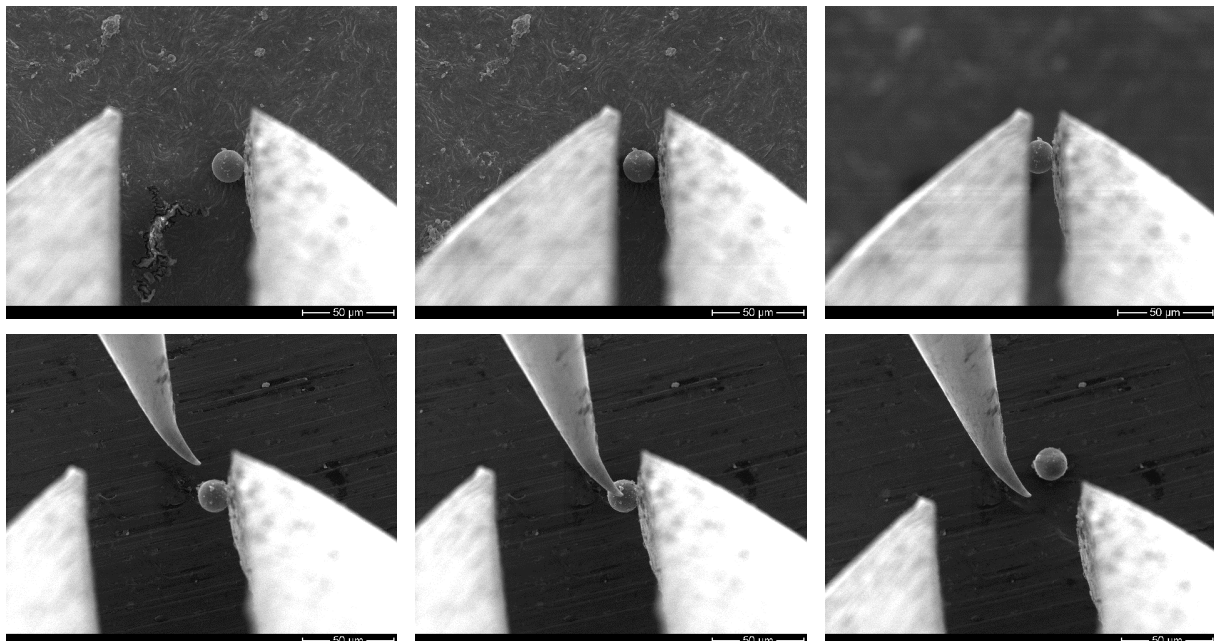


Figure 59: Grasping and brushing off a sphere with a diameter of 15 μm

4.4 DEM3: Cell Handling

The third demonstrator aims to show the capability of the Miniman-system to handle biological cells under the light microscope. For this, OLN-93 nerve cells stemming from the rat brain are sorted on an array of electrodes (see Figure 60). The electrical stimulation of a larger number of single cells or the recording of electro-

physiological signals of single cells requires the exact positioning of the cells on micro electrodes. Up to now it was a problem to exactly position one cell on each electrode. The cell handling demonstration now proves that this problem can be solved by the Miniman system in the future. Originally it was planned to sort the biological cells into microcuvettes, but currently there are more immediate applications for the sorting of cells on an electrode array.

The demonstration is specified as follows: The Miniman-III robot shall move to a user defined cell, pick it up, transport it to a user defined target position and place the cell with an accuracy of about 5 μm . Thus in this demonstration the Miniman-system works in a semi-automated mode. Besides the user defining the target position and the cell to grasp, the demonstrator should not need any further user intervention. During the whole operation the cell must not get damaged.

4.4.1 Hardware used for cell handling

The whole demonstration runs under a light optical microscope (Leica DM-RXA) which can be widely controlled by software. Thus it is possible for the controller *e.g.* to switch to a different objective, to adjust the light and to move the platform the robot operates on.

As sensors for the positioning of the robot and the tip of the pipette the global positioning and the local vision system (see Chapter 3.3.3, page 21) are used. Since the tip of the pipette is only positioned in two dimensions no sensor for the third dimension, like the laser triangulation in the lens assembly, is needed.

For the secure transportation of the cell a suction gripper has been developed which is integrated into the Miniman-III robot (see Figure 60). It consists of the standard 30 mm manipulator ball with an integrated suction mechanism and a disposable glass pipette (for details see Chapter 3.2.1, page 9). The glass pipettes are commercially available (Eppendorf, Germany). They have – except for the tip - an outer diameter of 1 mm and a total length of about 50 mm. The tip is shaped like a straight tube with a length of about 7 mm and a wall thickness of a few microns. The inner dimension of the tip can be ordered customised to the size of the respective cell species, and should be chosen slightly larger than the cells to be handled (*cf.* Chapter 3.2.1, page 9). In the project mostly pipettes with an inner tip diameter of 25 μm were used.

The suction mechanism is based on a piezo tube. Via a wire connection consisting of two thin wires it can be controlled by the robot system. The piezo suction mechanism allows the suction and release of defined liquid volumes: The maximum volume is about 5000 picolitres, the resolution about 20 picolitres. With the liquid flow cells can be positioned with a maximal inaccuracy of $\pm 6 \mu\text{m}$ (*calculated resolutions depending on the digital resolution of the robot system: 5V/256 steps*).

The demonstrator electrode array (Figure 60) has been structured on a glass substrate. It consists of 6 x 10 circular gold electrodes, each having a diameter of 40 μm . The distance between the electrodes is 110 μm . Starting from the electrodes, conductor paths lead to corresponding solder pads. The conductor paths are covered by a 10 μm polyimide layer for insulation. So the demonstrator array is already suitable for cell stimulation and electro-physiological measurements.

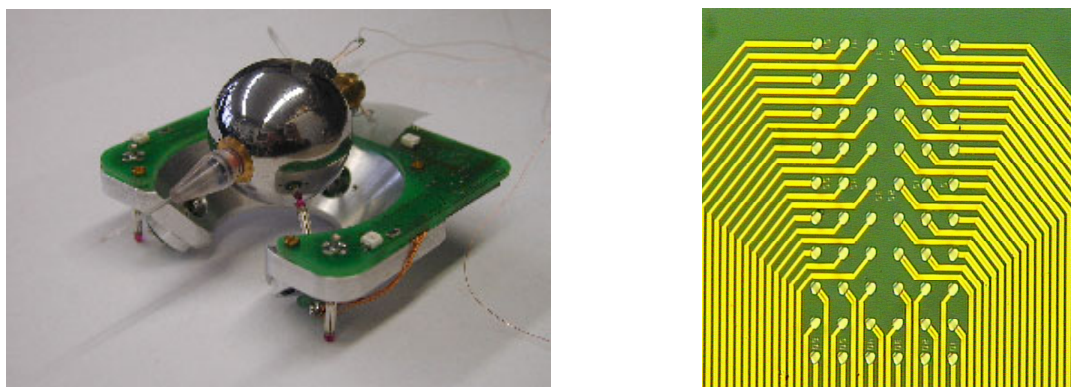


Figure 60: Miniman-III-2 robot equipped with the suction gripper (left); micromachined gold electrode array on glass (right)

4.4.2 Demonstration procedure

To guide the operator through the demonstration procedure, a multithreaded graphical user interface has been implemented (see Figure 61). For every step to be performed, it presents some information what is done and what the state of this step is. The operator has the possibility to interrupt and repeat a step of the procedure and if

everything fails, they can execute a step manually by using the robot in teleoperated mode (see Chapter 3.4.3, page 30).

After the demonstration application is started, the operator first has to move the microscope table to the position where they want the cell to be placed at. For this, the objective of the microscope can be changed to the zoom factor needed. After finding the desired position they have to click with the mouse at this position. The next action to take place is to move the microscope to a position where the desired cell can be observed. The cell is then marked for transportation by clicking at any point inside the cell with the mouse. The boundary of the cell is then detected by using the vision systems active contour method (see Chapter 3.3.3.2, page 23). The result is graphically presented to the operator so they can decide if the recognition of the cell boundary was successful. Afterwards, the boundary of the cell is used to create a template for the correlation tracking method. The last action required from the human operator is then to position the tip of the pipette in the field of view. Thereby they have to make sure that the tip of the pipette is at the same height as the cell.

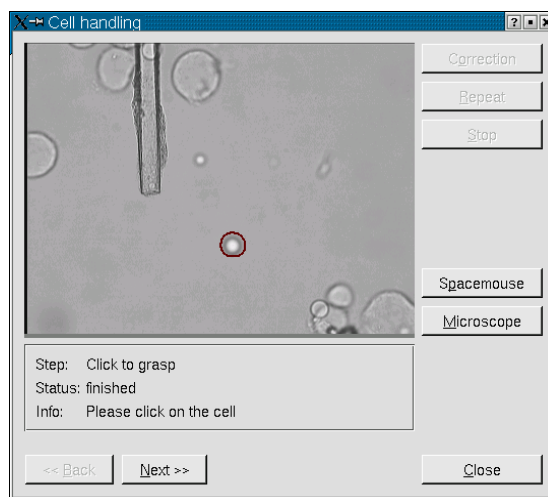


Figure 61: Graphical user interface for the cell handling demonstration

After the human operator has selected the desired cell and positioned the tip of the pipette in the field of view, the rest of the procedure runs automatically without any further interaction. First, the tip of the pipette is recognised using the vision method described in Chapter 3.3.3.5, page 26. To pick up the cell, Miniman then positions the opening of the pipette tip some pixels above the cell. During the whole positioning, not only the tip of the pipette is tracked but also the marked cell. This is because the movement of the pipette sometimes causes a movement of the cells in the suspension. If the position of the cell changed, the destination position is re-adjusted.

The next step is to suck in the cell. For this, the sucking power is at first increased rapidly to a medium value to get the cell detached. Then the sucking power is constantly increased to the maximum value. During the whole procedure, the cell is tracked in the image. After the cell is sucked in, the tip of the pipette is placed at the target position.

The last step after having placed the tip of the pipette near the target position is to blow out the cell and place it at the desired position. For this, the blowing power is slowly increased. To check if the cell has left the pipette a tracking of the template is attempted, which has been created during sucking in the cell, in front of the tip. When the error value of the tracking method is reasonably small, the cell is supposed to have left the pipette. Afterwards the cell is blown until it reaches the destination position.

4.4.3 Results

The tests of the cell handling demonstration show the flexibility and capability of the Miniman system. The automated positioning of the pipette tip within an accuracy of 10 μm was successfully shown. Also the automated grasping and releasing of a cell is possible.

Nevertheless, there are quite a lot of problems that tend to disrupt the successful cycle of the demonstration procedure. For example, the cell tracking is likely to fail if the cells have been in the suspension for too long a time. The cells absorb the water which results in a low contrast to the surrounding. In that case, the cell is still recognisable for a human operator but for the vision system the difference to the suspension around the cell is too less to track it successfully. Also when the cell is sucked into the pipette the vision system sometimes is able to track it and sometimes it loses it. This depends on things like other cells being stuck to the boundary of the pipette while having moved it through the suspension or some cells deforming when being sucked in, some not.

The closed-loop control using the local sensor system works fine, even when the zoom factor is changed. There had been some problems when positioning the pipette in the highest resolution (objective 20x). The tip of the pipette oscillated around the destination position because the movement was faster than the controller was able to get the next update of the pipette's position. This problem was circumvented by turning off updating of parameters not needed for local positioning and that are calculated from the global positioning system, *e.g.* the angle of the platform. This way, it was possible to successfully position the tip of the pipette.

Besides the positioning of the robot the automatic grasping and releasing of a cell has inherent problems. The biggest problem is, that the suction behaviour of the pipette is not always reproducible. Sometimes the cell drifts away in the pipette. To then get the cell out of the pipette again, it has to be blown out instead of placing it reliably in front of the pipette tip. Also a cell adhering to the ground is very hard to master with an automated system. For a human operator it is much easier to cope with this behaviour, because they can react much more flexibly to different situations.

To sum up the experience made with the cell handling demonstration it can be stated, that the Miniman system is in principle capable of doing the cell handling automatically. Although the reached automatism shows some instabilities and sometimes needs manual intervention of the operator, it shows that the Miniman system can be successfully extended by external sensors to run tasks (semi-)automated with the accuracy of circa 10 μm . The current state of the sensors, especially the missing sensor for the third dimension lets the automated procedure stand back to running the demonstration in teleoperated mode. To make the automated procedure a real alternative to teleoperation, still a lot of work would have to be done to stabilise the procedure and also to enhance the environmental conditions. For example, it would be necessary to make sure that the cells do not attach to the ground and that the volume and the bend of the suspension drop is kept constant.

4.5 Additional Subsystems

4.5.1 Force Feedback

In order to demonstrate the feasibility of force-feedback for micromanipulation an additional demonstrator was implemented. In this demonstrator objects of different materials are mounted on a purposely developed support. During grasping the operator feels the difference between soft and hard objects, using the commercially available haptic interface PHANTOM™.

For testing the force feedback, several tubes made of different materials will be gripped with the gripper (Figure 62). Together with the PHANTOM, one can clearly notice differences between the gripping forces. This effect can be used within a closed loop to grip different parts with different gripping forces (for example when gripping very soft parts or some biological materials). Force feedback is a very important feature of the developed gripper: the user quasi immerses into the micro world and gets a sense for the handled object.

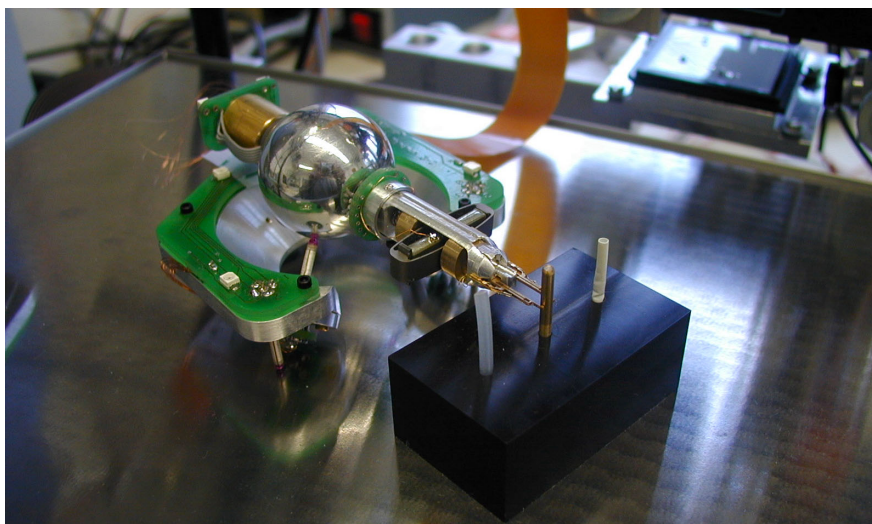


Figure 62: Miniman testing some different materials (Silicon, Brass, Elastomer)

4.5.2 Tactile Microsensor

An IDT-based tactile microsensor has been developed (see Chapter 3.3.2, page 18), which consists of an array of piezoresistive pressure detectors. The array has 64 elements arranged in 8 rows and 8 columns. The rows as well

as the columns have distances of 90 μm , the dimensions of one element are 55 μm x 55 μm . The overall size of the sensor is 900 μm x 900 μm .

The sensor design has been adapted to the shape of one of the fingers of the three finger gripper and the sensor has been integrated into the finger. The flexible design of the sensor allows an adaptation to other, even more complicated gripper shapes.

Hardware and software have been developed for preprocessing, calibration and representation of the sensor signals. The tactile image can be displayed on a computer monitor in real time. The sensor is controlled by row-column-encoding in order to minimise the number of wires – so for 64 tactile pixels only 16 connecting wires to the preprocessing hardware are necessary. The preprocessing hardware needs a power supply of ± 5 V.

The sensor allows the detection of shape and position of simply shaped micro objects like wires, needles and rings. The originally aspired linear sensor response could not be achieved sufficiently due to unpredictable resistance changes of the conductive silicone rubber pyramids, which form the contact elements of the sensor, but the binary response characteristics can be utilised for tactile object recognition.

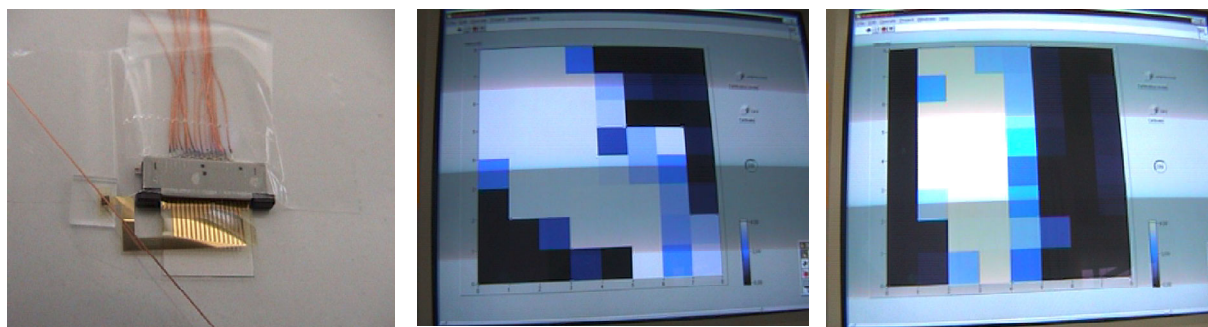


Figure 63: Tactile representation of a straight 200 μm wire (left) pressed diagonally (middle) or vertically (right) on the sensor surface

4.6 Benefits to Society

So far, much effort has been put on the production of the components, leading to remarkable scientific, technological and commercial advances in the Microelectronics, MEMS or MEOMS industries.

However, the complexity of the involved technologies implies a huge initial investment in the production facilities, limiting these products to niche markets where cost is not an essential issue or where very large production is possible.

In the electronics market today there is already a dangerous monopoly situation. Only few companies around the world can risk the necessary investments of billions of Euro, which would be needed especially for new micromechatronic products. In contrast to that, a competitive and sustainable growth would require that there is a competition not only between a small number of large enterprises commercialising new emerging technologies and products. Small and especially young companies need to be likewise given the chance to participate in these developments.

The results of the Miniman project are expected to make new systems possible which were to date discarded due to missing assembly and manipulation facilities. The flexible Miniman robot concept offers a versatile and innovative instrument to perform micro manipulations in a prototypical or small volume scale, either the experimental handling of biological tissue, the assembly of micromechanical prototypes or small series or a very convenient tool in observation techniques requiring vacuum.

Also, the development of new micro actuator structures and low-cost fabrication processes is an important aspect for miniaturisation of systems. The identification of the crucial parameters for high precision manipulation of miniaturised components is extremely important knowledge in the future progress towards nanotechnology. The system approach, *i.e.* the marriage between actuator structures and integrated circuits, intelligent piezoceramics, is an important trend that has been strengthened in this project.

Characterising the mechanical properties of tiny biological tissues and measuring some physiological parameters, such as pressure in micro blood vessels, is very important for research in biology, physiology, and biomechanics, and can even lead to clinical applications in such fields as diagnostics, minimally invasive surgery, dermatology, and cosmetics. Cells of the body are exposed to mechanical stresses and strains throughout life, and this is critical to the health and functions of various tissues and organs of the body. It is clear that micro techniques and

microrobotics will provide powerful means for the development of a novel generation of research instruments. In fact, a variety of laboratory apparatuses and microfabricated instruments have been developed recently for investigating cells and tissues properties by mechanical stimulation. In addition to basic research in biomechanics, miniaturised robotic instruments are fundamental tools for minimally invasive diagnostics and surgery. Perhaps the most critical factor in MIS (Minimally Invasive Surgery) is the severe reduction of sensory and dexterous manipulation capabilities of the surgeon. Restoring (or even augmenting) these capabilities by developing new “smart” surgical tools would have a major impact on the future of the whole field of MIS. In this sense, the Miniman concept can not only be used to deepen our understanding on the cellular level, but also can the results of the Miniman project be used to push the technological limitations which exist today for the assembly of MIS tools and thereby make new kinds surgical, diagnostic or prosthetic micro systems possible.

4.7 Conclusion

The Miniman Project comprised the development of two kinds of flexible mobile micro robots with their control systems as well as the development of new tools and sensors that are integrated in one system. This system grew up from a variety of single prototype components (simple mobile platforms, single micro grippers, etc.) to a whole working system. It must be admitted, that obviously it is still in a prototype stage. However, it is already a helpful tool for various micromanipulation tasks. By means of its intuitive teleoperation mode, it enables the user to work in the microworld. At the same time, the Miniman robots prove that the development of mobile microrobots is a promising approach to realise very small and flexible tools that are suitable for very different applications. The following overview makes the flexibility of the system evident:

Application	Size of the handled objects	consistency of the objects	shape of the objects	environment	employed micro tool	speciality
Assembly of a micro lens system (DEM1, p. 38)	1 000 - 2 300 μm	rigid	circular, spherical	(irrelevant)	microgripper with force feedback	0.25 mrad alignment
Handling tasks inside the SEM (DEM2, p. 42)	10 - 500 μm	soft and rigid	irregular	vacuum chamber of SEM	micro gripper, micro probe	nano positioning stage
Cell Handling (DEM3, p. 43)	20 μm	soft	irregular	light microscope stage	micro pipette	interaction with living cells

Table 1: Overview of the demonstrations

The demonstration of the micro lens assembly yet leads also to a negative finding. It shows, that mobile microrobots like Miniman are still not flexible enough to provide a solution for all kinds of “special” tasks. The lens alignment is an example of such a special task, that will always require very special solutions. Miniman can only be a “multi tool” for a limited set of micro manipulation tasks. However, for a special task it can be reasonable to integrate the Miniman principle in a special environment or combine it with a special device – as it was done in case of the Lens Alignment Unit, which is simply the manipulator unit of a Miniman III robot.

A further negative result is the conclusion that the current technology is not yet suitable for production tasks. This is due to the fact that the automation of the mobile microrobots is difficult, because a basic sensor system – the positioning – is still too susceptible. As it is based on advanced machine vision, it must be adapted carefully to the particular task and environment and fails if the conditions change. Furthermore, the system is presently too slow for any kind of serial or mass production. Only the production in very small batch sizes is practical. In that case the convenient teleoperation of the robots is currently more efficient than the adjustment of the vision system. However, the present stage of the positioning system nevertheless substantiates an important progress. It shows, that it is possible to use the high resolution of the microscopes for the positioning of mobile microrobots. For the use in industrial production, flexible robots must always be equipped with special tools. Consequently, if the vision system is regarded as a module belonging to these particular tools (to which it must be adjusted), the Miniman robots catch up with their larger conventional colleagues in industry. By means of their positioning system they can be automated *e.g.* by using teach-in methods as already realised. What is more, the functionality of the Miniman vision system goes beyond the teach-in automation by comprising the detection of the position of the objects to be grasped (vision: see Chapter 3.3.3, p. 21).



Figure 64: Size comparison of the Miniman robots

The successor robot Miniman V (see Chapter 4.1, p. 36 and Chapter 3.5.1.2, p. 33) is already in a stage comparable to Miniman III in the very beginning of the project (Figure 64). The fact that this tiny robot is already moving – using only 6 wires – is undoubtedly one of the main achievements of the project. The reduction of the number of wires by using onboard ICs enables such a small robot to move at all. For comparison, even the movement of the large Miniman III is disturbed by its big number of wires – not to mention the problems caused by the lot of tiny solder joints and the complexity of signal distribution to multiple robots (see Chapter 3.4.1, p. 28). The development of Miniman V paves the way to future swarms of such robots, which may be a further approach to make mass production at microscopic scale possible.

In a nutshell, the Miniman project has accomplished by and large its main goal – to develop microrobots that free humans from the tedious task of having to handle minuscule objects directly.

5. Exploitation: Eventual Commercialisation of Miniman

5.1 Definition of the “Product”

From the project results two main product families are envisaged in the exploitation plans:

- The Miniman robot as a multi-purpose (universal) laboratory tool (always ready for use)
 - for handling any kind of micro-objects under a light microscope, such as parts of micro system prototypes to be assembled during the development of such products.
 - for handling biological objects such as cells or tissue samples
 - for handling small objects inside the SEM
- The Miniman Smart piezoactuators units as a low voltage, high accuracy micro-nano-positioners.
 - For translation or tilt stages on nanotechnologies applications
 - Hexapod micropositioning system (for example optics elements or lasers sources)

5.2 Biological applications

The microrobot could be used for multistation single-cell diagnostics. The robot arm can trap biological entities (single cells, bacteria, multicellular organisms, *etc.*) from a sample and then transfer them sequentially to different measurement stations of a multisensor area. The dimension reduction of the cm^3 robot is an important advantage. The reduction of electrical contacts per element reduces the amount of dead (non-functional) area. This leads to the possibility of a large number of microrobots operated simultaneously on a small area for the parallel handling of cells. To extend the application range of the robot, it is possible to introduce parallel fingers treated with adhesion molecules, for improved parallel cell selection and transfer, or introduce electrodes for electrical measurements controlled by the same chip used for the driving of the piezo-legs/hands.

5.3 Mechanical applications under the light microscope

When one analyses the situation of micro systems today, it is clear that assembly is one of the crucial points. There are two main alternatives: Much effort is put in R&D of methods to completely avoid assembly of micro parts and special solutions are being developed, tailored to a specific microassembly task. A third alternative is only possible for products with a very small volume, being the manual assembly under magnifying glasses or microscopes, which is still being done for several micro products today.

At the same time, there is a large number of possible micro systems which are not developed and built today due to the lack of assembly facilities. This could be summarised in the sentence “we cannot assemble this, let’s think of something else”. If developers had a versatile tool for prototyping such products which also offers the option to automate parts of the assembly process, this would possibly lead to a vital impulse for the microsystems market.

5.4 SEM applications

Many experiments and studies going on at present, require the manipulation of fine objects. Often these objects are so small, fragile, or hard to handle in other ways, that these exercises must be done in the SEM. At present, good success has been shown in using one or even two Miniman robots inside the SEM. This allows precision handling of very delicate material under visual observation.

The application field of Miniman may be grouped into three principal areas:

Micro Mechanics, such as grasping and assembling operations with delicate miniaturized objects. There are however several other instruments on the market that aim in the same direction. None of them can really work in the range lower than 5 to 10 μm . Miniman has the potential operate in this range – partly because of the versatility of its modular design concept, and partly because of the gripper and tool strategy. The versatility manifests itself in a wide range of “tips”, or “tools” such as Micro Tweezers, Micro Pipettes *etc.*, and the addition of a “Helping Hand”. One and the same system may be assigned to a wide span of tasks within a single project.

Assisting Diagnosis Work on ICs and Wafers. According to experts from an industrial company who suggested the aforementioned test of breaking of a FIB machined micro object from an IC, this technique can save enormous amounts of time and expenses for the diagnosis of matrix material on to which the chip structure is laid down, and for the recognition of defects. There are several reasons to believe that once the operation comfort will have been improved during further development, this field of work may become the most effective marketing power for Miniman systems. There is room for varying complexity – from a simple, desktop controller operated unit to a large work station with fringe accessories for automatic or semi-automatic operation. Micro operations involving several Miniman units together on the same working platform have been suggested.

Environmental Sciences. Pollen grains, plant pollution, collection of radioactive fallout, aerosols, toxic materials *etc.* may be traced down in the SEM, and then taken to an analysis station within the same specimen chamber. The vacuum in the SEM is kept intact during a work session, where numerous specimens are screened, suspicious particles will be picked up for cataloguing, micro analysis, or other techniques. It must be understood, that such experiments are often done with special instruments, such as a so-called “Environmental Scanning Electron Microscope”. This applies especially to fresh biological material, and wet specimens. The environmental stage allows working at elevated pressure, thus keeping the plant or animal structure turgid over some long periods of time. These relatively new techniques allow even the study of biological and chemical processes – such as the growth of crystals – at a microscopic scale with the quality of electron microscopy. During such experiments it is very probable that the user would like to interact with the microscopic world – as it is possible with the Miniman system.

6. Deliverables

Deliverable	Responsible Partner	Type	Title	Milestone	where to find
D001	IPR	Report	Intermediate progress report	M1	IPR
D002	IPR	Report	Intermediate progress report	M2	IPR
D003	IPR	Report	Final report and demonstrations	M3	IPR
D101	IPR	Hardware	Prototype with tube-shaped piezoactuators	M1	IPR
D102	DMS	Hardware	Prototype with multilayered piezoactuators	M2	DMS
D103	IPR+DMS	Hardware	Prototype tube-shaped and multilayered piezoactuators	M2	IPR
D201	PRLE	Report	Specification of handling techniques (micromechanical)	M1	IPR
D202	IBMT	Report	Specification of handling techniques (biological)	M1	IPR
D203	IBMT	Hardware	Suction gripper for biological cells	M1	IBMT
D204	SSSA	Hardware	Two-fingered LIGA microgripper	M1	SSSA
D205	K&W	Hardware	Two-fingered gripper, SEM-suitable	M1	IPR
D206	IPR	Hardware	Two-fingered gripper, scissors-like	M1	IPR
D301	SSSA	Hard-/Software	Force microsensor (strain gauge or piezo, $\mu\text{N} - \text{nN}$)	M2	SSSA
D302	IBMT	Hard-/Software	Tactile microsensor (IDT-based)	M2	IBMT
D303	SHU	Software	Vision system for object recognition, tracking and 3D information	M2→M3	IPR
D401	SSSA	Hard-/Software	Hardware and Software interface for teleoperation	M1	IPR
D402	IPR	Software	GUI Software for telemanipulation	M1	IPR
D403	IPR	Software	Closed-loop position/force control	M2→M3	IPR
D404	IPR	Hard-/Software	Embedded parallel multiprocessor system (PMS)	M1	IPR
D405	SIC	Hardware	PCB including microprocessor and smart power ICs	M2→M3	DMS, SIC
D501	SSSA	Hardware	Gripper with integrated force sensor	M2	SSSA
D502	IBMT	Hardware	Gripper with integrated tactile sensor	M2	IBMT
D503	IPR+DMS	Hardware	Micromanipulating units with integrated gripper	M2	IPR
D504	IPR+DMS	Hardware	Micropositioning units with integrated micromanipulating unit	M2	IPR
D505	IPR+DMS+SIC	Hardware	Final microrobot system with an integrated PCB	M3	DMS, SIC
D506	IPR	Software	Control system with integrated pre-processing modules of sensors	M3	IPR
D507	IPR+DMS+SIC	Software	Control algorithms for piezoactuators with signal optimizing module	M2	DMS, SIC
D508	IPR	Software	Control system with integrated PMS and GUI	M3	IPR
DEM1	IPR+DMS	Hard-/Software, Chapter 4.2	Handling of micromechanical objects under light microscope	M3	IPR
DEM2	IPR+K&W	Hard-/Software, Chapter 4.3	Handling of micromechanical objects in an SEM	M3	IPR
DEM3	IPR+IBMT+SSSA	Hard-/Software, Chapter 4.4	Handling of biological objects under light microscope	M3	IPR
DEV	IPR	Report, Chapter 5	Evaluation of Miniman using the Demonstrators	M3	IPR

7. References

- [Barrow 77] H. G. Barrow, J. M. Tenenbaum, R. C. Bolles, H. C. Wolf. "Parametric correspondence and chamfer matching: Two new techniques for image matching". In *5th International Joint Conference on Artificial Intelligence*, Cambridge, CA, pp. 659-663. Carnegie Mellon University, 1977.
- [Breguet 96] Breguet, J.-M.; Pernet, E.; Clavel, R.: "Stick and slip actuators and parallel architectures dedicated to microrobotics"; *Proc. SPIE 2906*, Boston, pp. 13-24, 1996
- [Evans 93] A. C. Evans, N. A. Thacker and J. E. W. Mayhew. "The Use of geometric histograms for model based object recognition". *Proceedings of the 4th BMVC*, Guildford, 129-138, 1993.
- [Haynes 83] S. M. Haynes, R. Jain. "Detection of moving edges", *Computer Vision, Graphics and Image Proc.*, 21, 345-367, 1983.
- [Martel 01] Martel, Sylvain, Sherwood, Mark, Helm, Chad, Garcia de Quevedo, William, Fofonoff, Timothy, Dyer, Robert, Bevilacqua, John, Kaufman, Joshua, Roushdy, Omar, and Hunter, Ian; "Three-Legged Wireless Miniature Robots For Mass-Scale Operations At The Sub-Atomic Scale", Proceedings of the 2001 IEEE International Conference on Robotics & Automation, Seoul. Korea, May 2001
- [Miyazaki 97] Miyazaki, H. et al.: "Adhesive forces acting on micro objects in manipulation under SEM"; *Microrobotics and Microsystem Fabrication*, SPIE 3202, Pittsburgh, 1997, pp. 197-208
- [Shi 94] J. Shi and C. Tomasi. "Good features to track". *IEEE Conf. on Computer Vision and Pattern Recognition*, 593-600, 1994.
- [Tsai 87] R.Y. Tsai, "A Versatile Camera Calibration Technique for High-Accuracy 3D Machine Vision Metrology Using Off-the-Shelf TV Cameras and Lenses," *IEEE Journal of Robotics and Automation*, No. 4, August 1987

Publications of the Miniman Consortium

- [Amavasai 00a] Amavasai, B.P., Yates R.B. and Meikle, S., *Vision control for a MEMs robotic system*, Journal of Measurement and Control, 2000. [SHU]
- [Amavasai 00b] Amavasai, B.P., Meikle, S. and Yates, R.B.: A robust vision system for micro-object manipulation, Proceedings of SPIE Vol. 4194: Microrobotics and Microassembly II, Boston, USA, Nov. 5-6, 2000, pp. 112-120 [SHU]
- [Amavasai 01] Amavasai, B.P., Caparrelli, F., Selvan, A.N., Salem, B. and Travis, J.R., *A real-time machine vision system for micro-robotic manipulation*, Micro-robotics - Can Technology Outsmart Nature (poster), Institute of Materials, UK, 16 May 2001. [SHU]
- [Biehl 00] Biehl M.: A sensor with genuine feel, FhG research news No. 6-2000, Topic 2. [IBMT]
- [Buerkle 01a] Buerkle, A., Schmoeckel, F., Wörn, H., Amavasai, B.P., Caparrelli, F., and Travis, J.R., *A versatile vision system for micromanipulation tasks*, Proc. of the International Conference on Multisensor Fusion and Integration for Intelligent Systems (MFI 2001), pp.271-276, ISBN 3-00-008260-3, Baden-Baden, Germany, 20-22 Aug 2001. [SHU, IPR]
- [Buerkle 01b] Buerkle, A., Schmoeckel, F., Kiefer, M., Amavasai, B.P., Caparrelli, F., Selvan, A.N. and Travis, J.R., *Vision based closed-loop control of mobile microrobots for micro handling tasks*, Proceedings of SPIE Vol. 4568: Microrobotics and Microassembly III, Boston, USA, October 2001. [SHU, IPR]
- [Campolo 99] D. Campolo, A. Eisinger, A. Menciassi, G. Granieri, M.C. Carrozza, P. Dario "Force Control of a Micrograsper for Microassembly", *Proceedings of MME'99*, Gif-sur-Yvette, France, Sept. 27-28, 1999. [SSSA]
- [Carrozza 00] Carrozza M.C., Eisinger A., Menciassi A., Campolo D., Micera S., Dario P.: TOWARDS A FORCE-CONTROLLED MICROGRIPPER FOR ASSEMBLING BIOMEDICAL MICRODEVICES, Journal of Micromechanics and Microengineering, Volume 10, Number 2, June 2000, pp. 271-276 [SSSA]
- [Caparrelli 99] F. Caparrelli, P. Rocket and R. Yates "A Novel Approach to Nearest Neighbour Search in High Dimensional Spaces for 3D Object Recognition" UK Seventh IEE Conference on Image Processing and its Applications IPA99, Manchester, 12 - 15 July 1999. [SHU]
- [Dario 01] Dario P., Eisinger A., Menciassi A., Francabandiera P., Stefanini C., Scalari G., Carrozza M.C., "A micro-electro discharge machined, superelastic alloy micrograsper for micromanipulation", Proceedings of

- EUSPEN 2001, EUSPEN'S 2nd International Conference, Turin, ITALY, May 27-31, 2001, pp. 852-855 [SSSA]
- [Domingo 99] Domingo, J.; Puig-Vidal, M.; López, J.; Samitier, J. "Non-linear control system based in fuzzy logic technique applied to drive piezoactuators for microrobotic applications" IEEE Int. Conference on Emerging Technologies and Factory Automation (ETFA'99). Barcelona, October 1999 [EME]
- [Eisenberg 01] Eisenberg A., Scalari G., Mazzoni M., Menciassi A., Dario P., "Force-feedback Sensorized Microgrippers for a Micromanipulation Workstation", Proceedings of AISEM 2001, 6th National Conference on Sensors and Microsystems, February 5 – 7, 2001, Pisa, ITALY [SSSA]
- [Eisenberg 01] Eisenberg A., Menciassi A., Micera S., Campolo D., Carrozza M.C., Dario P.: PI FORCE CONTROL OF A MICROGRIPPER FOR ASSEMBLING BIOMEDICAL MICRODEVICES, IEE Proceeding Circuits, Devices and Systems, Special Issue on Microsystems Technology, in print [SSSA]
- [Fatikow 99a] S. Fatikow, A. Buerkle and J. Seyfried: Automatic Control System of a Microrobot-Based Microassembly Station Using Computer Vision, SPIE's International Symposium on Intelligent Systems & Advanced Manufacturing, Conference on Microrobotics and Microassembly, Boston, Massachusetts, USA, 1999, pp. 11-22 [IPR]
- [Fatikow 99b] S. Fatikow, J. Seyfried, S. Fahlbusch, A. Buerkle, F. Schmoeckel: "A Flexible Microrobot-based Microassembly Station", Proc. of the 7th IEEE International Conference on Emerging Technologies and Factory Automation (ETFA'99), Barcelona, Spain, October 18-22, 1999 [IPR]
- [Fatikow 00] Fatikow, S., Seyfried, J., Fahlbusch, St., Buerkle, A., and Schmoeckel, F.: A Flexible Micro-robot-Based Microassembly Station, Journal of Intelligent & Robotic Systems, 27, Kluwer Academic Publishers, Dordrecht, 2000, pp. 135-169 [IPR]
- [López 99] López, J.; Miribel-Catala, P.; Puig-Vidal, M.; Domingo, J.; Bota, S.; Samitier, J. "Sistemas de Control de actuadores piezoeléctricos para microrobots" SAAEI'99 (Sem. Anual Automática Electrónica Industrial). Madrid, Sept. 1999. [EME]
- [Meikle 00a] Meikle, S. and Yates, R.B.: Smart sensors: Lessons learned from computer vision, *Proceedings of SPIE Vol. 3990: Smart Electronics and MEMS*, California, USA, Mar. 6-8 2000 [SHU]
- [Meikle 00b] Meikle, S. and Yates, R.B.: Building Smarter Sensors - Lessons learned from computer vision, *Proceedings of IEEE Intelligent Vehicles Symposium 2000*, pp210-214, Detroit, USA, Oct. 2000 [SHU]
- [Menciassi 00] Menciassi A., Scalari G., Eisenberg A., Anticoli C., Tonet O., Carrozza M.C., Dario P., "Soft Tissue Characterization and Grasping by Micromanipulation with Force-feedback", BioMEMS and Biomedical Nanotechnology World 2000, Columbus, OH, September 23-26, 2000 [SSSA]
- [Menciassi 01a] Menciassi A., Scalari G., Eisenberg A., Anticoli C., Francabandiera P., Carrozza M.C., Dario P., "An instrumented probe for mechanical characterization of soft tissues", *Biomedical Microdevices*, 3:2, 2001, pp. 149-156 [SSSA]
- [Menciassi 01b] Menciassi A., Eisenberg A., Scalari G., Anticoli C., Carrozza M.C., Dario P., "Force Feedback-based Microinstrument for Measuring Tissue Properties and Pulse in Microsurgery", Proceedings of the 2001 IEEE International Conference on Robotics & Automation (ICRA2001), Seoul, KOREA -May 21-26, 2001, pp. 626-631, Winner of the Best Manipulation Paper Award [SSSA]
- [Menciassi 01c] Menciassi A., Eisenberg A., Mazzoni M., Scalari G., Dario P., "Handling AFM Cantilever Chips by a Force Feedback-Based Micromanipulation System", Proceedings of IEEE-NANO 2001, First IEEE Conference on Nanotechnology, 28-30 October 2001, Maui, Hawai (USA), pp. 157-160 [SSSA]
- [Meyer 00] Meyer, M. U., Kinkopf, T., Biehl, M., Beutel, H., Thielecke, H.: A Micropipette with Integrated Fluid Channels for Parallel Grasping and Transporting Single Living Cells, VDE World Microtechnologies Congress (MICRO.tec 2000) Sep. 25-27, 2000, Expo 2000, Hannover, Germany; Lecture and Proceedings (Vol. 2). A first collaboration with an interested industry partner could be reached [IBMT]
- [Pat IBMT] Patent application DE 100 00 691 A1: Micro-Nozzle-System [IBMT]
- [Puig-Vidal 01] Puig-Vidal, M., López-Sánchez, J., Miribel-Català, P., Montené, E., Bota, S. A., Samitier, J., Simu, U. and Johansson, S.: Smart power integrated circuits to drive piezoelectric actuators for a cm³ microrobot system, SPIE's 8th Annual International Symposium on Smart Structures and Materials, New Port Beach, California, March 4-8, 2001 pp. [SIC, DMS]
- [Saatchi 99] R. Saatchi, R. Yates, A. Bürkle and S. Fatikow "Image Recognition of Miniature Objects for Microassembly Station" Micro-Machines Europe MME'99, Paris 26-28 September 1999. [SHU, IPR]

- [Schmoeckel 00] Schmoeckel, F., Fahlbusch, St., Seyfried, J., Buerkle, A., Fatikow, S.: Development of a microrobot-based micromanipulation cell in an SEM, SPIE's International Symposium on Intelligent Systems & Advanced Manufacturing, Conference on Microrobotics and Microassembly, Boston, MA, USA, November 5-8, 2000, pp. 129-140 [IPR]
- [Seyfried 00] Seyfried, J., Fatikow, S., Fahlbusch, St., Buerkle, A., and Schmoeckel, F.: Manipulating in the Micro World: Mobile Micro Robots and their Applications, 31st Int. Symposium on Robotics (ISR 2000), Montreal, Canada, May 14-17, 2000, pp. 102-107 [IPR]
- [Simu 99] Simu, U. and Johansson, S., Multilayer piezoceramic microactuators formed by milling in the green state, Proceedings of the SPIE Vol. 3892: Int. Symp. on Microelectronics and Micro Electro Mechanical Systems, Surfers Paradise, Australia, 1999 [DMS]
- [Simu 01a] Simu, U. and Johansson, S., A monolithic piezoelectric miniature robot with 5 DOF, Transducers'01, Munich, Germany, 10-14 June, 2001 [DMS]
- [Simu 01b] Simu, U. and Johansson, S.: Evaluation of a monolithic piezoelectric drive unit for a miniature robot, Submitted to Sensors and Actuators A (Physical) 2001 [DMS]
- [Simu 01c] Simu, U. and Johansson, S.: Design and fabrication of a miniature robot with monolithic piezoelectric drive units, Submitted to Journal of Micromechanics and Microengineering, 2001 [DMS]
- [Wörn 01] Heinz Wörn, Ferdinand Schmoeckel, Axel Buerkle, Josep Samitier, Manel Puig-Vidal, Stefan Johansson, Urban Simu, Jörg-Uwe Meyer, Margit Biehl: From decimeter- to centimeter-sized mobile microrobots - the development of the Miniman system, SPIE 's International Symposium on Intelligent Systems and Advanced Manufacturing, Conference on Microrobotics and Microassembly, Boston, MA, USA, October 28 - November 2, 2001, pp. 175-186 [IPR]

8. Outlook

As described in this report, a lot of new and exciting results have been achieved during the Miniman project. Several new tools have been developed to master the requirements of the fascinating micro world. New generations of Miniman-robots like Miniman III and IV have been created. Miniman V even advances the system towards the again smaller nano world.

In general, the project has extended the knowledge of fabrication and evaluation of micro technology. The results obtained give clear indication about parameters and steps the which are important for further miniaturisation, for example miniature actuators. Furthermore, the technology of the piezo suction gripper offers new possibilities for the handling of tiny liquid volumes. Together with the micromachined transparent micropipettes, new opportunities arise not only for the handling of cells or other microscopic particles, but also for the dispensing and mixing of very small liquid volumes. A first industry partner has already been interested in a dispensing application of the micro pipettes.

A special knowledge has been gained on the fabrication of microelectrodes on thin polyimide foil. The development of the microfabrication process with two metallic layers and very fine structures smaller than 10 μm , as it has been used for the fabrication of the tactile sensor, has deepened the understanding in this area. This process can be used not only for the development of tactile sensors, but also for other applications, where very small electrodes in two layers are needed. The existence of the tactile sensor demonstrators in combination with the graphic display offers access to further collaborations with industry partners concerning customised tactile sensor developments; first contacts have already been established.

Various issues regarding the use of vision feedback in real-time were addressed in the Miniman project. This has led to the design and implementation of a new software development platform, called Mimas, which was introduced earlier in this report. The package is licensed under a free software licence and it will be publicly released in the near future. It is hoped that this package will provide a framework for future development of real-time vision algorithms.

Many techniques that have been specifically developed for the Miniman project are likely to be applicable to future projects in various fields such as robotic control, 2D and 3D industrial assembly, biological manipulation and testing of MEMS devices.

With the results of the Miniman-project in mind, we can look forward into an even smaller world, namely into the nano-world. This means particles of about 0.1mm downwards. Therefore, a new task must be defined. The aim should be to bridge the gap between Miniman's world and molecular world which is today accessible only using

techniques like atomic force microscopes. One goal could be the development of a multi-microrobot manipulating system prototype used to handle micrometre-sized objects in the so-called “mesoscopic range” as well as smaller, “nano-scale” objects.

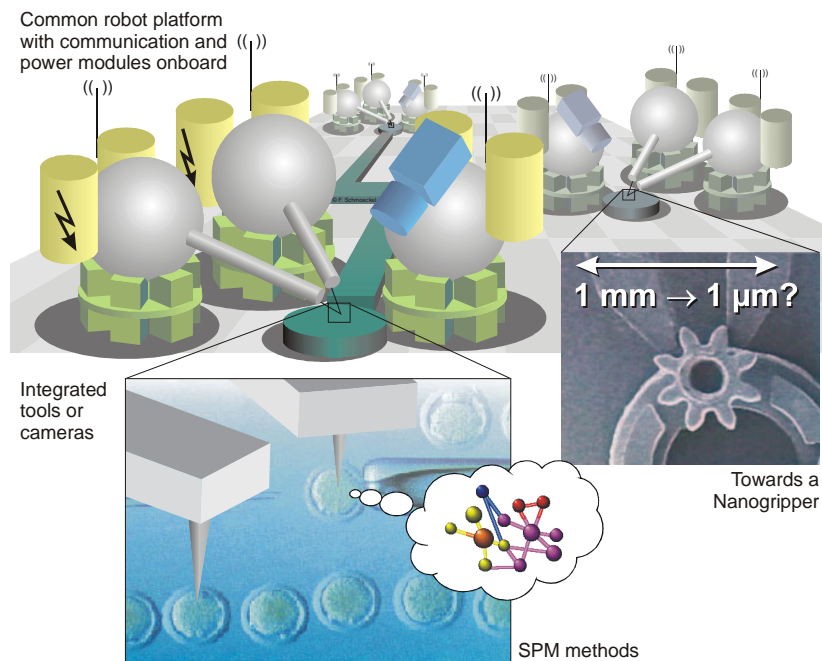


Figure 65: Future application: thinking towards nano-range

In his 1959 famous talk - “*There’s plenty of room at the bottom*” - Richard Feynman suggested that one of the ways to reach the bottom (the molecular world) was to build small robots that in turn would build even smaller robots. The first step towards the “bottom” has already been taken with the development of scanning probe microscopes (SPM). However, even though these *manipulators* can handle atoms, they are themselves physically large. The interaction of a *small* robot with the molecular world would take advantage of the scaling down effects. Both the operation frequency and the motion accuracy would improve but perhaps, more importantly, the robot would be more sensitive to the molecular interactions thus improving our knowledge of the molecular world. In comparison with other visions, Feynman’s talks have been regularly revisited and have shown to precede the technical development in the microsystems area. Today, one of the main research areas in the nano-range is the investigation of biological issues, *e.g.* manipulations in the molecular scale. Such SPM-based manipulations could be a starting point of a future project, capitalising on the successes of the Miniman-project.

Last but not least, the integration work within the Miniman Project has strengthened the European network regarding partners with complementary technology. This effect would be intensified by launching a new joint project, where all the partners could involve their own scientific expertise.